



Article

# Metamitron and Shade Effects on Leaf Physiology and Thinning Efficacy of *Malus × domestica* Borkh

Nídia Rosa <sup>1,\*</sup>, Glória Àvila <sup>2</sup>, Joaquim Carbó <sup>2</sup>, Wim Verjans <sup>3</sup>, Isabel Pereira Pais <sup>4,5</sup>, Anabela Bernardes da Silva <sup>6</sup>, Luísa Louro Martins <sup>1</sup>, Miguel Pedro Mourato <sup>1</sup>, Luísa Cristina Carvalho <sup>1</sup>, Paula Scotti-Campos <sup>4,5</sup>, Joan Bonany <sup>2</sup>, Luís Asín <sup>7,\*</sup>, José Cochicho Ramalho <sup>5,8,\*</sup> and Cristina Moniz Oliveira <sup>1,\*</sup>

<sup>1</sup> Linking Landscape, Environment, Agriculture and Food (LEAF), Instituto Superior de Agronomia (ISA), Universidade de Lisboa, 1349-017 Lisbon, Portugal; luisalouro@isa.ulisboa.pt (L.L.M.); mmourato@isa.ulisboa.pt (M.P.M.); lcarvalho@isa.ulisboa.pt (L.C.C.)

<sup>2</sup> IRTA EEA Mas Badia, La Tallada d'Empordà, 17134 Girona, Spain; gloria.avila@irta.cat (G.À.); joaquim.carbo@irta.cat (J.C.); joan.bonany@irta.cat (J.B.)

<sup>3</sup> Pcfuit Research Station, BE-3800 Sint-Truiden, Belgium; wim.verjans@pcfuit.be

<sup>4</sup> Unidade de Investigação em Biotecnologia e Recursos Genéticos (UIBRG), Instituto Nacional de Investigação Agrária e Veterinária, I.P. (INIAV), 2784-505 Oeiras, Portugal; isabel.pais@iniav.pt (I.P.P.); paula.scotti@iniav.pt (P.S.-C.)

<sup>5</sup> Unidade de Geobiociências, Geoengenharias e Geotecnologias (GeoBioTec), Faculdade de Ciências e Tecnologia, Universidade Nova de Lisboa, 2829-516 Caparica, Portugal

<sup>6</sup> Biosystems & Integrative Sciences Institute (BioISI), Faculdade de Ciências da Universidade de Lisboa, 1749-016 Lisboa, Portugal; arsilva@fc.ul.pt

<sup>7</sup> IRTA Fruitcentre, PCiTAL, Park of Gardeny, Fruitcentre Building, 25003 Lleida, Spain

<sup>8</sup> Plant Stress & Biodiversity Lab, Centro de Estudos Florestais (CEF), Instituto Superior Agronomia (ISA), Universidade de Lisboa, 2784-505 Oeiras, Portugal

\* Correspondence: nidia.helena.rosa@gmail.com (N.R.); luis.asin@irta.cat (L.A.); cochichor@mail.telepac.pt or cochichor@isa.ulisboa.pt (J.C.R.); crisoniz@isa.ulisboa.pt (C.M.O.)

Received: 11 November 2020; Accepted: 4 December 2020; Published: 7 December 2020



**Abstract:** Thinning strategies, namely shade or photosynthetic inhibitors, rely on the reduction of carbon supply to the fruit below the demand, causing fruit abscission. In order to clarify the subject, seven field trials were carried out in Lleida, Girona, and Sint-Truiden (2017 + 2018), using orchards of 'Golden' and 'Gala' apple trees. At the stage of 9–14-mm fruit diameter, four treatments were implemented: (A) CTR-control, trees under natural environmental conditions; (B) SN-shaded trees, trees above which shading nets reducing 50% of irradiance were installed 24 h after metamitron application date—without application of metamitron—and removed after five days; (C) MET-trees sprayed with 247.5 ppm of metamitron; (D) MET + SN-trees submitted to the combined exposure to metamitron application and shading nets. Low radiation significantly increased metamitron absorption (36–53% in the three locations in 2018) and reduced its degradation. Net photosynthesis and stomatal conductance were strongly reduced in all treatments, with minimum values 2 days after spraying (DAS) and incomplete recovery 10 DAS in MET + SN. All treatments resulted in leaf sucrose and sorbitol decreases, leading to a negative carbon balance. SN and MET + SN promoted the highest thinning efficacy, increasing fruit weight and size, with MET + SN causing over-thinning in some trials. Leaf antioxidant enzymes showed moderate changes in activity increases under MET or MET + SN, accompanied by a rise of glutathione content and a reduction in ascorbate, however without lipid peroxidation. This work shows that environmental conditions, such as cloudy days, must be carefully considered upon metamitron application, since the low irradiance enhances metamitron efficacy and may cause over-thinning.

**Keywords:** carbohydrate balance; fruit abscission; photosynthesis; reactive oxygen species; RuBisCO; shading

---

## 1. Introduction

Annual apple (*Malus domestica* Borkh.) production has increased steadily, becoming the third most produced fruit in the world in 2018, with 86 million metric tons [1]. In times in which farmers must meet the high quality criteria of the market, thinning is one of the most important management practices to achieve apple quality for fresh consumption and, consequently, economic sustainability. The thinning strategy needs to be adjusted every year, depending on the fruit set and desired crop load. However, the results can strongly differ between years and regions [2,3] in some cases, in an unpredictably manner.

Nowadays, there are several widely used chemical thinning agents, including met amitron. This triazinone herbicide is a systemic xylem-translocated compound, which inhibits photosystem (PS) II by blocking the electron transfer between the primary and secondary quinones, leading to the closure of the reaction centres and disrupting thylakoid electron transport [4,5], which, ultimately, will greatly reduce photosynthetic carbon fixation [4,6]. The use of shading nets is another thinning technique used in several crops and in organic farming, namely in grapes [7] and apples [8,9]. The role of light in apple production was frequently studied [10]. Studies have shown that by significantly reducing light availability to apple trees through shading, for a certain number of days at a specific post-bloom period, fruit drop will be promoted due to a restriction in carbohydrate availability caused by the limited leaf C-assimilation [8,11–13]. Under light, the photochemical reactions provide reducing power, nicotinamide adenine dinucleotide phosphate (NADPH), and chemical energy molecules, adenosine triphosphate (ATP), both of which are essential for sugar production resulting from the carboxylation capability of ribulose-1,5-bisphosphate carboxylase/oxygenase (RuBisCO), and Calvin-Benson cycle functioning.

Both met amitron and shading nets can significantly reduce the photosynthetic rate in apple trees, by inhibiting the photosynthetic apparatus [14], and by reducing the amount of light energy reaching the chloroplast, which will reduce glucose and sorbitol synthesis [15]. This last monosaccharide is necessary to form sucrose, the main form of transport of assimilated carbon within the plant, from source to sink organs [16]. Additionally, sorbitol synthesis could also be affected. This polyol represents the highest percentage of non-structural sugars in apple trees, being as well a primary product of photosynthesis in the Rosaceae family [17]. However, unlike sucrose, which is synthesized and utilized by leaves of all ages, sorbitol is synthesized in leaves, but is metabolized only in sink tissues [18].

It is increasingly accepted that thinning efficacy is directly related to carbohydrate balance, leading to the development of several models for thinning estimation [19–22]. A carbohydrate surplus will lead to a lower fruit drop rate, while a deficit will result in fruit growth decline and stimulation of the abscission zone formation, promoting the efficacy of the thinning compound [22]. Meteorological conditions also play a very important role on the tree's carbon balance [22–24], thus with the potential to change the efficacy of met amitron from no thinning at all to an over thinning effect [25]. A study of the interactions between cloudy weather, fruit set, and chemical thinning application methods is therefore relevant to unveil the variability of thinning efficacy.

Several abiotic stressors that impair the photochemical energy use can increase cell oxidative conditions [26]. Met amitron also reduces the light energy use by blocking PSII function, what might contribute to an over reduction of the photosynthetic apparatus, thus increasing the probability of electron acceptance by molecular oxygen and a greater reactive oxygen species (ROS) production in the chloroplast [27–29]. In fact, plant strategies to cope with abiotic stresses normally involve a wide set of responses, being the control of reactive oxygen species (ROS) one of the most important [30].

This involves enzymatic and non-enzymatic antioxidants that direct and indirectly allow the plants to cope with the ROS imbalance, thus avoiding oxidative damage. The ascorbate-glutathione pathway, whose enzymes act directly on ROS, such as  $H_2O_2$ , and also regenerate reduced forms of non-enzymatic antioxidants (e.g., ascorbate, glutathione), is a very important way of maintaining the plant oxidative status.

On the other hand, the reduction of irradiance reaching the photosynthetic apparatus by means of shading nets would reduce the probability of oxidative stress occurrence. Therefore, the evaluation of the balance of oxidative stress and their control mechanisms in apple leaves might contribute to improve the understanding regarding the implications of the single or combined use of metamiltron and shade treatments. Overall, in this study, we characterize some physiological and biochemical responses of the apple leaf/tree to the single and combined use of these thinning agents. It is also our goal to evaluate the effect of low irradiance (cloudy days) in fruit abscission and how it can enhance metamiltron thinning efficacy, in order to provide the grower with more detailed information about time intervals with negative carbon balance which, depending on the crop load goal, acts as perfect thinning windows or may cause over-thinning.

## 2. Materials and Methods

### 2.1. Plant Material and Experimental Design

#### 2.1.1. Plant Material

Trials were performed in experimental orchards of *Malus × domestica* in Lleida and Girona (Spain) in 2017, and in Lleida, Girona, and Sint-Truiden (Belgium) in 2018. In Lleida, trials were carried out in the experimental orchards of IRTA, Mollerussa, northeast of Spain ( $41^{\circ}61'96.37''$  N/ $0^{\circ}87'06.66''$  E, 245 m altitude), using 'Gala Brookfield' trees, grafted on M.9 NAKB, spaced  $4\text{ m} \times 1.4\text{ m}$ , with a canopy height of 3 m, planted in 2003, with 'Fuji' as pollinator. In Girona, trials were carried out in IRTA Más Badia, northeast of Spain ( $42^{\circ}03'12.97''$  N/ $3^{\circ}03'46.13''$  E, 12 m altitude), using 'Golden Reinders' trees, grafted on M9 NAKB, spaced  $3.8\text{ m} \times 1.1\text{ m}$ , with a canopy height of 2.5 m, planted in 2003, with 'Granny Smith' as pollinator. In Sint-Truiden, trials were performed on the orchards of PCFruit Research Station-Proefcentrum Fruitteelt vzw, Belgium ( $50^{\circ}45'49''$  N/ $05^{\circ}09'26''$  E, 96 m altitude), using 'Golden Delicious' trees, grafted on M9, spaced  $3.5\text{ m} \times 1.5\text{ m}$ , with a canopy height of 3 m, planted in 2005, without pollinator.

For biochemical evaluations, the leaves were cleaned with a water-wet tissue before being frozen in liquid  $N_2$ . All leaves were then finely powdered with a mortar and pestle in liquid  $N_2$  and kept at  $-80^{\circ}\text{C}$  until analysis.

#### 2.1.2. Treatment Implementation

The shade treatment was imposed by using shading nets installed at 4 m high, covering the whole canopy until the ground, on Eastern and Western sides of tree, which reduced the photosynthetic photon flux density (PPFD) by 50%, evaluated by two Watchdog 3670I Silicon pyranometers placed above and under the net and a Testo 1000 Microstation (Spectrum Technologies Inc., Aurora, CO, USA) (Figure 1). The shading nets were placed 24 h after metamiltron application, to ensure that absorption was not affected by low radiation and/or temperature, maintained during 5 days, and were removed at the end of the fifth day.

Spraying of metamiltron, the active ingredient of Brevis<sup>®</sup> (ADAMA, Telaviv, Israel), was carried out always in the early morning with the recommended dose of  $247.5\text{ ppm per }1000\text{ L ha}^{-1}$ , using a hand-gun sprayer. The moment of single application was determined by average fruit diameter: between 9–10 or 13–14 mm in 2017 (in two distinct trials) and around 14 mm in 2018.

Four treatments were established: (A) CTR-control, corresponding to trees under natural environmental conditions; (B) SN-shaded trees, trees above which shading nets were installed

24 h after metamitron application date—without application of metamitron—and removed after five days; (C) MET-trees sprayed with 247.5 ppm of metamitron, applied as referred above; (D) MET + SN-trees submitted to the combined exposure to metamitron application (MET) and shading nets placement during 5 days after metamitron application (SN). Metamitron and/or shade treatments were implemented between the 18th of April and the 18th of May.



**Figure 1.** Shading nets installed in Girona, IRTA Más Badia orchards, in 2017.

To monitor the environmental conditions in each trial, temperature and relative humidity sensors placed in both sides of the blocks and in the middle (with and without shading net), in each case, in the upper (2 m) and lower (1 m) level of the trees. In Lleida, six Testo 177-h1 (Testo, Titisee-Neustadt, Germany) were used; in Girona, six EasyLog USB Data Logger (Lascar Electronics, Wiltshire, UK) were used; and six Testo 174H sensors (Spectrum Technologies Inc., Aurora, CO, USA) were used in Sint-Truiden.

The initial number of flower clusters was similar among treatments (data not shown). Four blocks were established along two rows of the orchard, each 150-m long, in a randomized complete block design, with several trees between them with no treatments assigned and no observations done. The blocks were interspersed within the two rows, assuring that there were no blocks for observation immediately on the side row, avoiding the edge effect. Each block was constituted by four trees per treatment, but only the 2 central ones were used, performing a total of 8 observed trees per treatment, except in Girona 2017, where 4 trees per treatment was used.

## 2.2. Metamitron Leaf Analysis

In 2017, leaf samples for metamitron and desamino-metamitron concentration were collected 2, 4, 6, and 9 days after spraying (DAS) in leaves of the 9–10 mm fruit diameter trial in Lleida, whereas in 2018, the samples were taken 2 DAS in all locations. Each sample was a pool of three shoot leaves from the top, middle, and bottom part of each tree, with three samples being taken from the Eastern and three from Western side of the canopy, for a total of six repetitions per treatment.

Metamitron extraction was conducted according to the QuEChERS method [31] using 500 mg fresh weight (FW) of frozen leaf powder and 3 mL of acetonitrile. The samples were shaken manually for 1 min, after which, 1.95 g of extraction Supel™ QuE Citrate Extraction Tube (Sigma-Aldrich, St. Louis, MO, USA) was added, containing 1.2 g of magnesium sulfate, 0.3 g of sodium chloride, 0.15 g of sodium citrate dibasic sesquihydrate, and 0.3 g of sodium citrate tribasic dehydrate. The samples were further shaken manually for 1 min and centrifuged ( $6000\times g$ , 5 min, 4 °C). An aliquot of 1.2 mL of the supernatant was transferred to a 2 mL Supel™ QuE Verde clean-up tube (Sigma-Aldrich, St. Louis, MO, USA), vortexed, and further centrifuged ( $6000\times g$ , 5 min, 4 °C). The obtained supernatant was filtered with a polytetrafluoroethylene (PTFE) 0.45  $\mu\text{m}$  filter, and injected. Standard curves were used for the quantification of metamitron (Sigma-Aldrich, St. Louis, MO, USA) and desamino-metamitron-desamino (LGC Standards, Middlesex, MA, USA).

### 2.3. Leaf Gas Exchanges

Leaf gas exchanges measurements included net photosynthesis rate ( $P_n$ ), and stomatal conductance to water vapour ( $g_s$ ), and were obtained using a portable Infra-Red Gas Analyzer (IRGA) LCi Ultra Compact Photosynthesis System (ADC BioScientific, UK), under ambient conditions of irradiance, temperature (between 17–25 °C), humidity, and CO<sub>2</sub> supply (400 ± 20 ppm), between 10–12 h. In each of the four blocks, two evaluations in the Eastern and two in the Western side of the canopy were performed, in recently fully developed shoot leaves at ca. 1.5 m height, totaling 8 leaves per treatment. In 2017, gas exchanges measurements were taken in Lleida and Girona 2, 4, 6, 9, and 11 DAS, while in 2018, they were taken in Sint-Truiden 2, 5, and 10 DAS.

### 2.4. Ribulose-1,5-Bisphosphate Carboxylase/Oxygenase Activity

For ribulose-1,5-bisphosphate carboxylase/oxygenase (RuBisCO, EC number: 4.1.1.39), one shoot leaf per tree, making a total of four samples per treatment, were sampled 5 DAS in Sint-Truiden, in 2018, and from each leaf, ten 0.5 cm<sup>2</sup> leaf discs (80 mg FW) were cut, immediately frozen in liquid N<sub>2</sub> and stored at −80 °C.

#### 2.4.1. Extraction

Leaf material was homogenized in a cooled pestle and mortar, along with quartz sand, and 1% (*w/v*) insoluble polyvinylpyrrolidone, in 1 mL of ice-cold extraction buffer 50 mM Bicine-KOH (pH 8.0), containing 1 mM EDTA, 5% (*w/v*) polyvinylpyrrolidone, 6% polyethylene glycol (PEG4000), 10 mM DTT, 50 mM β-mercaptoethanol, and 1% (*v/v*) protease inhibitor cocktail for plant extracts (Sigma Aldrich, Germany). The homogenates were centrifuged (14,000× *g*, 5 min, 4 °C), and the clear supernatant was immediately used for RuBisCO activities evaluation by the incorporation of <sup>14</sup>CO<sub>2</sub> into acid-stable products at 25 °C, following [32].

#### 2.4.2. Total Activity Evaluation

The assay medium for enzyme activity determination contained 100 mM Bicine-NaOH pH 8.2, 40 mM MgCl<sub>2</sub>, 100 mM NaHCO<sub>3</sub> and 10 mM NaH<sup>14</sup>CO<sub>3</sub> (7.4 kBq μmol<sup>−1</sup>). For total activity ( $V_t$ ), 450 μL of assay medium and 25 μL of extract was incubated for 3 min at 25 °C for carbamylation, after which 25 μL of 0.4 mM RuBP was added. The reaction was allowed for 1 min, after which it was stopped with 200 μL 10 M HCOOH (formic acid). Samples were then kept overnight in an oven at 70 °C until total medium evaporation and the residue rehydrated with 500 μL of ultrapure water and 5 mL of scintillation liquid (Ultima Gold<sup>TM</sup>, Sigma-Aldrich, St. Louis, MO, USA). Radioactivity due to <sup>14</sup>C incorporation in the acid-stable products was measured by liquid scintillation counting using a scintillation spectrometer LS 7800 (Beckman Instruments Inc., Indianapolis, IN, USA).

### 2.5. Leaf Non-Structural Sugars

In 2017, sampling was performed between 11:30 and 13:00, at 2, 4, 6, and 9 DAS only from the 9–10-mm application in Lleida for starch analysis, while in 2018, that was done at 2, 5, and 10 DAS for soluble sugars in all trials. In 2017, four repetitions per treatment, one per block, in pools of 2 shoot leaves and 2 spur leaves were used. In 2018, the number of repetitions was increased to six.

#### 2.5.1. Soluble Sugars

Quantification of sucrose, fructose, glucose, and sorbitol was based on the method described by [33] using 150 mg FW frozen leaf material. The separation of sugars was performed using a Sugarpak1 column (300 × 6.5 mm, Waters) at 90 °C, using H<sub>2</sub>O (containing 50 mg EDTA-Ca L<sup>−1</sup>) as eluent, at a flow rate of 0.5 mL min<sup>−1</sup> in an HPLC system equipped with a refractive index detector (Model 2414, Waters, Milford, MA, USA). Standard curves of each sugar were used for quantification.

### 2.5.2. Starch

Starch quantification was performed based on a previous report [34] using ca. 150 mg FW frozen leaf material. The glucose derived from starch was enzymatically determined, with readings at 340 nm using a spectrophotometer UV-VIS Helios (Thermo Fisher, Waltham, MA, USA).

## 2.6. Leaf Oxidative Status Evaluation

Sampling was performed 5 DAS in Sint-Truiden, in 2018, between 10–12 h. Each sample was a pool of three shoot leaves (one sample per block, totaling 4 samples per treatment) that was frozen in liquid nitrogen and stored at  $-80\text{ }^{\circ}\text{C}$  until analysis.

### 2.6.1. Lipoperoxidation and $\text{H}_2\text{O}_2$ Content

Sample extraction was performed using 200 mg FW frozen material, homogenized with 2.0 mL of 0.1% trichloroacetic acid (TCA), and centrifuged ( $12,000\times g$ , 15 min,  $2\text{ }^{\circ}\text{C}$ ). Lipid peroxidation was estimated by measuring malondialdehyde (MDA) content, using the thiobarbituric acid (TBA) method, as described by [35]. After extraction, 4 mL of 20% TCA containing 0.5% TBA was added to a 1 mL aliquot of the supernatant. This mixture was heated ( $95\text{ }^{\circ}\text{C}$ , 30 min) followed by quick cooling in an ice bath and centrifugation ( $10,000\times g$ , 15 min,  $2\text{ }^{\circ}\text{C}$ ). The amount of MDA was calculated from the coefficient of absorbance at 532 nm after subtracting the non-specific absorption at 600 nm. The extinction coefficient  $155\text{ mM}^{-1}\text{ cm}^{-1}$  for MDA was used.

Hydrogen peroxide ( $\text{H}_2\text{O}_2$ ) content was measured using the method described previously [36]. To a 50  $\mu\text{L}$  aliquot of the supernatant obtained in the extraction, 959  $\mu\text{L}$  of 100 mM phosphate buffer, pH 7.6, and 1 mL of 1 M potassium iodide were added. The absorbance of the supernatant was measured at 390 nm and for quantification, we used a standard curve of hydrogen peroxide (0, 1.1, 2.2, 3.3, 4.4, and 5.5  $\mu\text{g mL}^{-1}$ ).

### 2.6.2. Antioxidative Enzyme Assays

For catalase (CAT), guaiacol peroxidase (GPOD), superoxide dismutase (SOD), and glutathione reductase (GR) 200 mg FW frozen material were homogenized in 2 mL of cold 100 mM Tris-hydrochloric acid (HCl) buffer, pH 7.8, containing 3 mM dithiothreitol, 1 mM EDTA, 2% (*w/w*) insoluble PVPP and centrifuged ( $12,000\times g$ , 20 min,  $4\text{ }^{\circ}\text{C}$ ). For ascorbate peroxidase (APX) activity determinations, 10 mM of ascorbate was added to the previously described solution. For glutathione peroxidase (GPX) activity determinations, 0.1% (*w/v*) Triton X-100, 5 mM cysteine, and 0.1 mM Phenylmethanesulfonyl fluoride were added to the solution described for CAT, SOD, GPOD, and GR. The resulting supernatant was used for determination of enzymatic activity (4 replicates were used for each determination). Absorbance was measured in a Hitachi (U-2000 UV/Vis, Hitachi, Japan) spectrophotometer, at ca.  $25\text{ }^{\circ}\text{C}$ . The enzyme activity was expressed as unit  $\text{g}^{-1}$  FW.

#### Catalase

CAT activity (EC 1.11.1.6) was evaluated as described earlier [37], with some changes, by following the decrease in absorbance at 240 nm for 2 min in a solution containing 10 mM of  $\text{H}_2\text{O}_2$  in 50 mM phosphate buffer, pH 7.0. Enzymatic activity was defined as the consumption of 1  $\mu\text{mol H}_2\text{O}_2$  per min and per  $\text{cm}^3$  using a coefficient of absorbance of  $39.4\text{ mM}^{-1}\text{ cm}^{-1}$ .

#### Guaiacol Peroxidase

Guaiacol peroxidase (GPOD) activity (EC 1.11.1.7) was determined following the increase of absorbance at 470 nm, according to a modification of methodology described previously [38], using a reaction mixture containing 30 mM 2-methoxyphenol (guaiacol) and 4 mM  $\text{H}_2\text{O}_2$  in 0.2 M sodium acetate buffer, pH 6.0. Enzymatic activity was defined as the consumption of 1  $\mu\text{mol}$  of guaiacol per min and per mL using a coefficient of absorbance for tetraguaiacol of  $26.6\text{ mM}^{-1}\text{ cm}^{-1}$ .

### Glutathione Reductase

Glutathione reductase (GR) activity (EC 1.8.1.7) was determined using a modified [39] method, measuring the increase in absorbance at 412 nm, using a reaction mixture containing 3 mM 5,5'-dithio-bis(2-nitrobenzoic acid) (DTNB), 2 mM nicotinamide adenine dinucleotide phosphate (NADPH) and 20 mM oxidized glutathione (GSSG) in 100 mM phosphate-ethylenediaminetetraacetic acid (EDTA) buffer, pH 7.6, and 1mM EDTA. Enzymatic activity was defined as the consumption of 1  $\mu\text{mol}$  of GSSG per min and per mL using a coefficient of absorbance of  $6.2 \text{ mM}^{-1} \text{ cm}^{-1}$ .

### Superoxide Dismutase

Superoxide dismutase (SOD) activity (EC 1.15.1.1) was determined using a modified [40] method, following the variation of absorbance at 550 nm, using a reaction mixture with 0.1 mM EDTA, 0.5 mM Xantine and 0.05 mM of ferricytochrome c in 100 mM phosphate buffer, pH 7.6, and  $1 \text{ U mL}^{-1}$  xantine-oxidase. Enzymatic activity was defined as  $\mu\text{mol}$  of ferricytochrome c reduction by superoxide radical  $\text{min}^{-1}$ .

### Ascorbate Peroxidase

Ascorbate peroxidase (APX) activity (EC 1.11.1.11) was determined according to a previous study [41], in a reaction mixture containing 0.25 mM ascorbate and 0.3 mM hydrogen peroxide in 50 mM phosphate buffer, pH 7.0, following the decrease in absorbance at 290 nm. Enzymatic activity was defined as the consumption of 1  $\mu\text{mol}$  ascorbate per min and per mL using a coefficient of absorbance of  $2.8 \text{ mM}^{-1} \text{ cm}^{-1}$ .

### Glutathione Peroxidase

Glutathione peroxidase (GPX) activity (EC 1.11.1.9) was determined according to [42], in a reaction mixture containing 1.14 mM sodium chloride, 2 mM reduced glutathione, 2.5 mM hydrogen peroxide, 2 mM NADPH in 50 mM Tris-HCl buffer, pH 7.9. Enzymatic activity was defined as the glutathione-peroxidase necessary to reduce 1  $\mu\text{mol}$  NADPH per min and per mL at room temperature using a coefficient of absorbance of  $6.2 \text{ mM}^{-1} \text{ cm}^{-1}$ .

### 2.6.3. Non-Enzyme Antioxidants Quantification

For glutathione and ascorbate evaluations, samples of 100 mg of powdered frozen leaf were homogenized in 0.5 mL of ice-cold 6% meta-phosphoric acid, pH 2.8, containing 1 mM EDTA and 1% activated charcoal powder for chlorophyll removal. Homogenates were centrifuged ( $27,000 \times g$ , 15 min,  $4^\circ\text{C}$ ), and the obtained supernatant was stored at  $-80^\circ\text{C}$  prior to glutathione and ascorbate analysis.

### Glutathione

The quantification of reduced (GSH) and oxidized (GSSG) glutathione was based on the method described previously [43]. Total glutathione was measured spectrophotometrically at 412 nm in a microplate reader Synergy HT (BioTek Instruments, Winooski, VT, USA). Oxidized glutathione (GSSG) was measured by incubating the diluted sample in 0.5% 2-vinylpyridine for 1 h at  $25^\circ\text{C}$  and then proceeding as described above. Reduced glutathione (GSH) was determined as the difference between total glutathione and GSSG.

### Ascorbate

The quantification of ascorbic (AsA) and dehydroascorbic (DAsA) acids was based on a method adapted from a previous study [44], as described earlier [45]. Absorbance was recorded at 525 nm in a microplate reader Synergy HT (BioTek Instruments, Winooski, VT, USA). Concentration of AsA was determined using a calibration curve of AsA in the range of 10–60 mM prepared in 5% metaphosphoric

acid. The concentration of DAsA was calculated by subtracting the AsA concentration measured from the total ascorbate assayed.

### 2.7. Yield Parameters

All fruits were picked from each observed tree at harvest, on one time. The number of fruits per tree, yield, fruit weight, and distribution per fruit size was determined using a commercial sort machine (Maf Roda Agrobotic, Montauban Cedex, France).

### 2.8. Statistical Analysis

The various measured and calculated parameters were subjected to an analysis of variance, through a one-way ANOVA, to evaluate the differences between treatments on one single day after spraying, or a two-way ANOVA to evaluate the differences between the four treatments, across the several days after spraying, followed by a Tukey's test for mean comparisons. Each ANOVA was performed independently for each of the trials. For metamidron leaf concentration and non-structural sugars data analysis six samples were used and a completely randomized design analysis was performed. A 95% confidence level was adopted for all tests. The statistical analysis was performed using Statistix 9 (Analytical Software, Tallahassee, FL, USA).

## 3. Results

### 3.1. Environmental Conditions

A brief characterization of the environmental conditions in the seven performed trials is shown in Table 1. Global irradiance values were quite homogeneous within all trials. The 2018 trial in Girona stands out due to the higher night temperature values, above 14 °C, registered before the application. In all the other trials carried out, the sensors installed inside and outside the shading nets showed no relevant differences neither in humidity nor in temperature ( $\approx 5\%$  and  $0.5\text{ }^{\circ}\text{C}$ , respectively), meaning that the only different parameter was irradiation, which was reduced by half.

**Table 1.** Summary of meteorological conditions  $\pm$  SE in trials performed in each year and location and fruit diameter at the time of metamidron application: average of daily irradiance 5 days after spraying (DAS) ( $\text{MJ m}^{-2}$ ), average night-time temperature from 20:00–8:00 h ( $^{\circ}\text{C}$ ), 5 nights before and after spraying, and average air relative humidity (%) during the 3 h prior to spraying in natural environmental conditions (Control) and under the shading nets (SN).

Location	Fruit Diameter (mm)	Global Irradiance $\text{MJ/m}^2$ —5 Days after		Night Temperature $^{\circ}\text{C}$ —5 Nights before	Night Temperature $^{\circ}\text{C}$ —5 Nights after	Diurnal Temperature $^{\circ}\text{C}$ —5 Days after	Relative Humidity %
		Control	SN	Control	Control	Control	Control
2017							
Lleida	$10 \pm 0.4$	$24.8 \pm 2.1$	$12.4 \pm 1.2$	$11.1 \pm 0.4$	$7.9 \pm 0.5$	$14.3 \pm 0.4$	$71.7 \pm 1.1$
	$13 \pm 0.4$	$17.7 \pm 1.9$	$8.8 \pm 0.9$	$7.5 \pm 0.5$	$8.0 \pm 0.6$	$13.0 \pm 0.3$	$56.0 \pm 3.4$
Girona	$9 \pm 0.7$	$20.7 \pm 1.8$	$10.4 \pm 0.9$	$9.3 \pm 0.6$	$10.4 \pm 0.4$	$13.3 \pm 0.4$	$47.3 \pm 3.1$
	$13 \pm 0.2$	$19.2 \pm 1.2$	$9.6 \pm 0.6$	$10.4 \pm 0.4$	$8.2 \pm 0.7$	$11.0 \pm 0.4$	$46.3 \pm 3.0$
2018							
Lleida	$14 \pm 0.3$	$17.5 \pm 1.2$	$8.8 \pm 0.6$	$10.2 \pm 0.2$	$11.8 \pm 0.5$	$12.7 \pm 0.5$	$61.5 \pm 2.1$
Girona	$14 \pm 0.3$	$19.3 \pm 1.3$	$9.7 \pm 0.6$	$15.5 \pm 0.7$	$11.8 \pm 0.4$	$14.6 \pm 0.3$	$69.1 \pm 1.9$
Sint-Truiden	$14 \pm 0.4$	$22.1 \pm 1.4$	$11.1 \pm 0.7$	$11.5 \pm 0.2$	$11.6 \pm 0.3$	$14.3 \pm 0.6$	$60.5 \pm 1.7$

### 3.2. Metamidron Absorption and Degradation to Desamino-Metamidron

To evaluate the metamidron impacts it is crucial to determine its absorption by the leaves and its permanence/degradation along time. For the applied dose, MET treatment reached  $2\text{ mg g}^{-1}$  dry



weight (DW) in leaf biomass of metamiltron 2 DAS, but the combined MET + SN treatment showed a significantly higher content of 1/3 considering an average of the three locations (Figure 2).

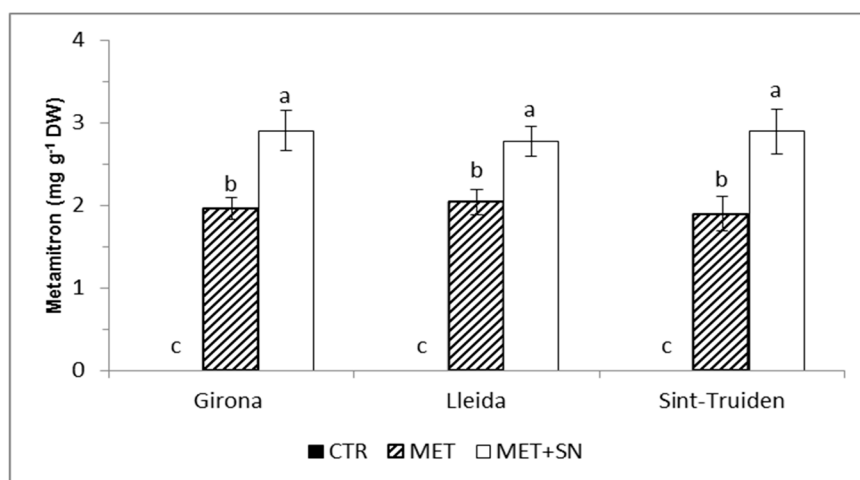


**Figure 2.** Metamiltron content ( $\text{mg g}^{-1}$  DW), evaluated 2 DAS, in the trials of 2018 in Girona ('Golden Reinders'), Lleida ('Gala Brookfield') and Sint-Truiden (Golden Delicious'). For each parameter, the mean values  $\pm$  SE ( $n = 6$ ) followed by different letters express significant differences between treatments within each cultivar after a Tukey's HSD test ( $p$ -value  $\leq 0.05$ ). SN-Shading net; MET-Metamiltron.

The pattern of variation of MET and MET + SN was similar during the whole experiment for desamino-metamiltron, the main degradation product of metamiltron (Figure 3). However, for MET in a higher extent (usually more than double) along this period. Desamino-metamiltron highest values were observed at 6 DAS, decreasing afterwards in both treatments.

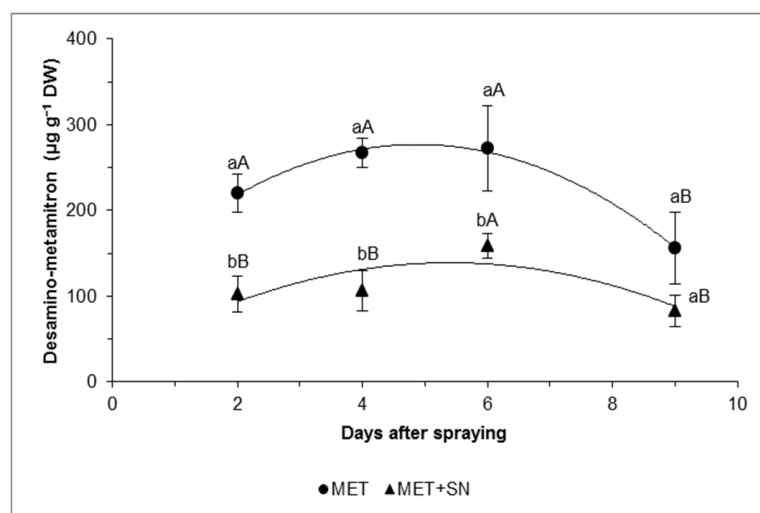


**Figure 3.** Desamino-metamiltron content evaluated 2, 4, 6, and 9 DAS, for metamiltron with (MET + SN-▲) or without (MET-●) shading nets, in the trials of 2017, in Lleida ('Gala Brookfield'). For each parameter, the mean values  $\pm$  SE ( $n = 8$ ) followed by different letters express significant differences between treatments within each day (a and b), or between days within each treatment (A and B), after a Tukey's HSD test ( $p$ -value  $\leq 0.05$ ). SN-Shading net; MET-Metamiltron, DAS-Days after spraying.

### 3.3. Leaf Gas Exchanges

$P_n$  and  $g_s$  were similar among the treatments applied at 9–10 mm and 13 mm, allowing combining the data from those trials for each site (Figure 4). The recovery period was evaluated 9 DAS in the

9–10 mm fruit diameter metamitron application and 11 DAS in the 13 mm, and the analysis made separately (data not shown).

Overall, the treatments of metamitron and/or shade imposed a reduction on  $P_n$  and  $g_s$  until 6 DAS in both locations. In detail, SN significantly reduced  $P_n$  and  $g_s$  in Lleida (50% and 55%) (Figure 4b) and Girona (24% and 53%) (Figure 4c,d), respectively, 2 DAS. Lowered  $P_n$  and  $g_s$  values were mostly maintained 4 DAS, but a strong increase to values close to their controls was observed 6 DAS, that is, just one day after shade removal.

MET significantly reduced  $P_n$  at 2 and 4 DAS, 35 and 42%, and 39 and 80%, in Lleida and Girona, respectively, as compared to their control values on the same days. Moreover, although in Lleida the  $P_n$  values in the MET treatment were invariant until 6 DAS, in Girona, minimum  $P_n$  values were observed 4 DAS with a tendency to recovery afterwards. MET further caused  $g_s$  reductions in both sites, with maximal declines at 4 DAS of 42 and 40% of their respective controls.

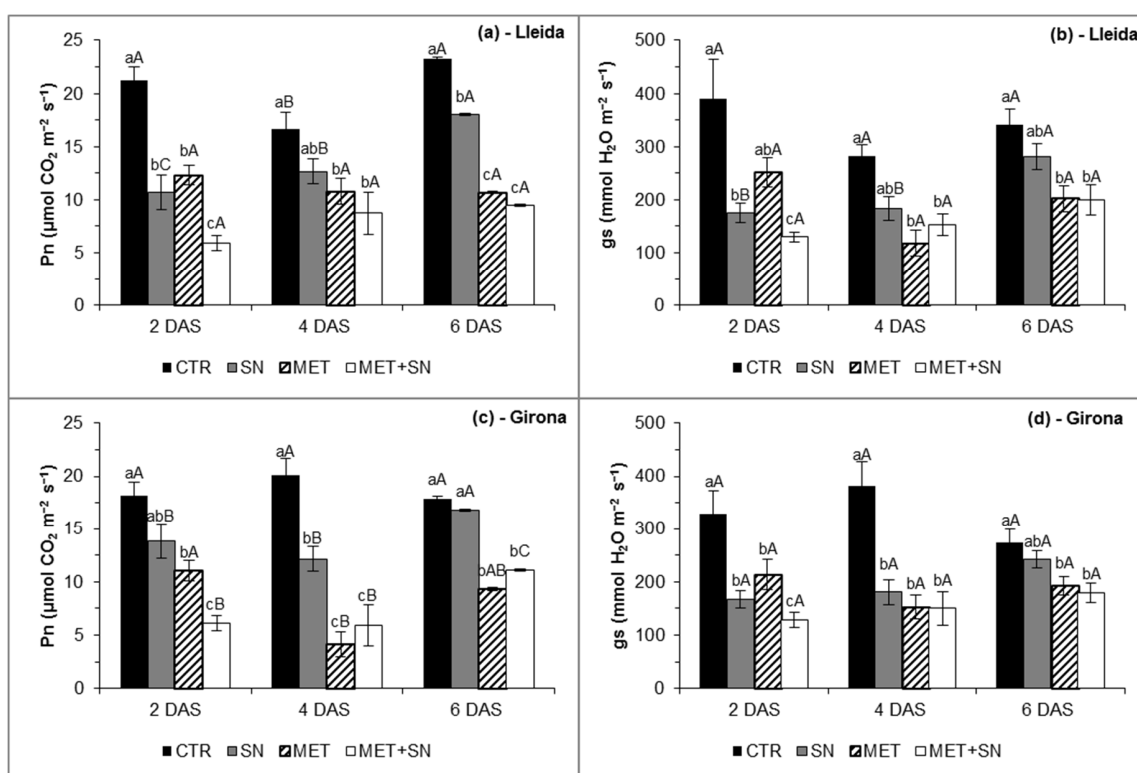


**Figure 4.** Net CO<sub>2</sub> gas exchange ( $P_n$ ) ( $\mu\text{mol CO}_2 \text{ m}^{-2} \text{ s}^{-1}$ ) (a,c) and stomatal conductance to water vapor ( $g_s$ ) ( $\text{mmol H}_2\text{O m}^{-2} \text{ s}^{-1}$ ) rate (b,d), in Lleida and Girona, respectively, evaluated 2, 4, and 6 days after shade (DAS) installation, in the 2017 trials in Lleida ('Gala Brookfield') and Girona ('Golden Renders'). Shading nets were removed 5 DAS. For each parameter, the mean values  $\pm$  SE ( $n = 16$ ) followed by different letters express significant differences between treatments within each day (a–c), or between days within each treatment (A, B, and C), after a Tukey's HSD test ( $p$ -value  $\leq 0.05$ ). SN-Shading net; MET-Metamitron, DAS-Days after spraying.

The MET + SN treatment caused the most significant reduction in  $P_n$  and  $g_s$  2 and 4 DAS, to half of CTR values, or even to a greater extent. Furthermore, 2 DAS, the values were usually lower than those of MET. Although a tendency to recover was observed after shade removal, in MET + SN treatment,  $P_n$  and  $g_s$  did not differ from those from MET alone, showing that 6 DAS metamitron was leading the impact of MET + SN treatment. Evaluation of the leaf gas exchanges for longer periods in the Lleida experiments showed that at 9 DAS MET plants still represented 30% ( $P_n$ ) and 25% ( $g_s$ ) lower values than CTR, but 11 DAS differences between treatment become absent (data not shown). Measurements performed in Sint-Truiden in 2018 were in line with those of Lleida in 2017, although at 10 DAS

(thus, five days after the removal of the shading nets), only the MET + SN maintained significant reduced  $P_n$  values (data not shown).

### 3.4. RuBisCO Activity

Total activity of RuBisCO ( $V_t$ ) was significantly reduced to less than half as CTR, in MET and MET + SN treatments, without significant differences between them (Table 2).

**Table 2.** RuBisCO total activity ( $V_t$ ) ( $\mu\text{mol CO}_2 \text{ m}^{-2} \text{ s}^{-1}$ ) evaluated 5 DAS, in the trial of 2018 in Sint-Truiden ('Golden Delicious'). For each parameter, the mean values  $\pm$  SE ( $n = 4$ ) followed by different letters express significant differences between treatments within each cultivar after a Tukey's HSD test ( $p$ -value  $\leq 0.05$ ). SN-Shading net; MET-Metamitron.

$V_t$ ( $\mu\text{mol CO}_2 \text{ mg}^{-1} \text{ Chl}$ )		
CTR	20.7 $\pm$ 1.4	a
SN	19.8 $\pm$ 0.9	a
MET	8.4 $\pm$ 0.3	b
MET + SN	8.3 $\pm$ 0.8	b

### 3.5. Leaf Sugars

SN treatment significantly reduced sucrose content in Lleida and Girona at 2 DAS (36 and 53%) and in all locations at 5 DAS (between 47–62%) (Table 3). A similar trend was observed for sorbitol, although less striking than sucrose, significant in Sint-Truiden at 2 DAS (36%) and in all locations at 5 DAS (between 22–34%). Glucose also showed significant a reduction in Lleida, with 21% less content than CTR. At 10 DAS, there were no differences from CTR likely due to the removal of the nets at 5 DAS.

The MET treatment showed only non-significant impacts 2 DAS. However minimum levels were reached at 5 DAS, and sucrose (34–59%), fructose (24–44%), sorbitol (22–24%), and total sugars (21–24%) were frequently significantly reduced, as compared to CTR. At 10 DAS, Lleida trees still presented reduced content of sucrose, whereas Sint-Truiden all evaluated sugars presented values similar to control.

The combined MET + SN treatment showed a consistent tendency to cause greater impact than the single treatments in all days and trials, although minimum values were reached at 5 DAS. By this time, MET + SN treatment promoted significant reductions in sucrose (62–78%), sorbitol (29–42%), and total sugars (30–38%) in the three locations, as compared to the control. In addition, this treatment resulted in 70% less glucose in Lleida and 53 and 64% less fructose content in Lleida and Sint-Truiden, respectively, comparing to the respective controls. At 10 DAS, the trees still presented a reduced content of sucrose of 80% compared to the CTR.

**Table 3.** Main soluble sugars content ( $\text{mg g}^{-1} \text{ DW}$ ) of apple leaves: sucrose, glucose, fructose, sorbitol, and total sugars at 2, 5, and 10 DAS in Lleida ('Gala Brookfield'), Girona ('Golden Reinders') and Sint-Truiden ('Golden Delicious') in the 2018 trials. Shading net was removed 5 DAS. For each parameter, the mean values  $\pm$  SE ( $n = 6$ ) followed by different letters express significant differences between treatments within each day (a, b, and c), or between days within each treatment (A and B), after Tukey's HSD test ( $p$ -value  $\leq 0.05$ ). No letters indicate a  $p$ -value  $> 0.05$ . SN-Shading net; MET-Metamitron, DAS-Days after spraying.

	2 DAS									
	Sucrose		Glucose		Fructose		Sorbitol		Total	
	Lleida									
CTR	16.6 $\pm$ 1.2	aA	31.5 $\pm$ 2.8	aA	2.9 $\pm$ 0.5	aA	91.0 $\pm$ 5.3	aA	141.9 $\pm$ 7.9	aA
SN	10.7 $\pm$ 1.0	bA	31.3 $\pm$ 2.9	aA	2.4 $\pm$ 0.5	aA	76.8 $\pm$ 4.2	aA	120.9 $\pm$ 6.9	aA
MET	12.7 $\pm$ 0.5	abA	31.6 $\pm$ 2.3	aA	2.3 $\pm$ 0.2	aB	68.1 $\pm$ 9.9	aA	114.6 $\pm$ 13.5	aA
MET + SN	10.9 $\pm$ 1.7	bA	32.0 $\pm$ 3.8	aA	1.7 $\pm$ 0.6	aA	79.8 $\pm$ 6.4	aA	124.4 $\pm$ 12.1	aA

Table 3. Cont.

2 DAS										
	Sucrose		Glucose		Fructose		Sorbitol		Total	
<b>Girona</b>										
CTR	19.6 ± 1.9	aA	48.4 ± 4.0	aA	2.3 ± 0.7		88.9 ± 7.8	abA	151.3 ± 12.9	abA
SN	9.3 ± 0.9	bcA	37.9 ± 1.5	abA	3.1 ± 0.4		71.3 ± 4.5	bA	121.6 ± 5.9	bA
MET	14.2 ± 2.0	abA	40.5 ± 4.1	abA	4.8 ± 0.7		101.0 ± 10.1	aA	168.3 ± 15.1	aA
MET + SN	6.8 ± 1.0	cA	35.8 ± 2.1	bA	3.6 ± 0.6		65.3 ± 6.0	bA	111.5 ± 8.4	bA
<b>Sint-Truiden</b>										
CTR	24.8 ± 3.0	aA	44.7 ± 4.7		6.2 ± 0.6	aA	120.0 ± 10.9	aA	195.8 ± 14.6	aA
SN	21.1 ± 8.6	aA	33.7 ± 5.0		4.4 ± 0.3	aA	77.4 ± 4.6	bB	136.6 ± 10.5	bA
MET	17.5 ± 1.0	aA	42.6 ± 4.4		6.2 ± 0.8	aA	99.4 ± 6.3	abA	165.7 ± 10.7	abA
MET + SN	11.9 ± 1.1	aA	41.0 ± 2.7		5.5 ± 1.2	aA	78.4 ± 4.4	bB	136.7 ± 8.5	bA
<b>5 DAS</b>										
	Sucrose		Glucose		Fructose		Sorbitol		Total	
<b>Lleida</b>										
CTR	12.9 ± 0.9	aB	36.3 ± 1.6	aA	3.2 ± 0.2	aA	87.4 ± 2.6	aA	138.9 ± 4.9	aA
SN	4.9 ± 0.5	cB	28.6 ± 1.8	bA	2.2 ± 0.4	abA	58.5 ± 2.7	cB	75.1 ± 2.6	cB
MET	6.7 ± 0.5	bB	31.6 ± 1.7	abA	1.8 ± 0.1	bB	69.4 ± 2.5	bA	109.5 ± 2.3	bA
MET + SN	2.9 ± 0.6	bcB	10.5 ± 0.6	cA	1.5 ± 0.1	bA	50.9 ± 2.7	cB	85.9 ± 3.5	cB
<b>Girona</b>										
CTR	15.5 ± 1.4	aA	28.1 ± 2.1	aB	3.1 ± 0.5		70.5 ± 3.7	aB	117.2 ± 6.5	aB
SN	6.1 ± 0.2	bB	25.1 ± 1.8	aB	3.2 ± 0.2		46.6 ± 2.0	bB	78.9 ± 3.0	bB
MET	6.7 ± 1.4	bB	25.5 ± 3.3	aB	2.9 ± 0.8		53.8 ± 5.7	abB	89.0 ± 10.4	bB
MET + SN	5.2 ± 0.5	bA	23.1 ± 1.1	aB	2.2 ± 0.3		42.8 ± 4.5	bB	73.3 ± 5.0	bB
<b>Sint-Truiden</b>										
CTR	16.6 ± 1.1	aB	39.7 ± 3.1		5.0 ± 1.1	aA	85.4 ± 4.4	aB	146.7 ± 8.7	aB
SN	7.7 ± 1.1	bcB	35.2 ± 1.7		3.4 ± 0.5	abA	66.4 ± 4.0	bB	112.1 ± 6.3	bB
MET	11.0 ± 1.5	bB	30.8 ± 1.1		3.8 ± 0.7	abB	66.9 ± 3.9	bB	112.5 ± 5.0	bB
MET + SN	6.4 ± 0.6	cB	35.7 ± 2.6		1.8 ± 0.3	bB	59.0 ± 2.7	bC	102.8 ± 4.8	bB
<b>10 DAS</b>										
	Sucrose		Glucose		Fructose		Sorbitol		Total	
<b>Lleida</b>										
CTR	10.8 ± 0.8	aB	14.2 ± 2.5	aB	2.5 ± 0.4	aA	89.9 ± 4.8	aA	117.4 ± 7.8	aA
SN	7.9 ± 0.8	abA	11.2 ± 1.5	aB	2.2 ± 0.4	aA	87.0 ± 2.7	aA	108.4 ± 2.8	aA
MET	5.0 ± 0.8	bcB	15.6 ± 1.0	aB	3.7 ± 0.7	aA	80.9 ± 4.0	aA	101.4 ± 4.3	aA
MET + SN	2.1 ± 0.3	cB	12.7 ± 1.3	aB	3.4 ± 0.6	aA	75.1 ± 5.4	aA	95.3 ± 6.6	aAB
<b>Sint-Truiden</b>										
CTR	15.3 ± 1.8	aB	45.9 ± 2.2		3.4 ± 0.6	aA	102.6 ± 4.0	aAB	167.1 ± 7.3	aAB
SN	11.2 ± 0.8	aB	38.5 ± 4.8		3.2 ± 0.2	aA	93.8 ± 3.4	aA	140.7 ± 4.9	aA
MET	12.5 ± 0.6	aB	37.5 ± 2.5		3.0 ± 0.5	aB	103.6 ± 6.7	aA	156.6 ± 9.0	aA
MET + SN	12.4 ± 1.0	aA	35.4 ± 3.0		3.5 ± 0.2	aAB	98.7 ± 4.0	aA	150.0 ± 7.5	aA

Regarding the insoluble sugar starch, all treatments promoted content reduction up to 6 DAS (significantly until 4 DAS). Maximal declines (greater than 70%) were observed at 4 DAS, as compared to the respective control value (Table 4). The starch content was similar among the treatments at 9 DAS, although related to a strong starch reduction in CTR plants, as compared with the previous days.

**Table 4.** Leaf starch content ( $\text{mg g}^{-1}$  DW) at 2, 4, 6, and 9 DAS (9–10-mm application trial) in the trial of 2017, in Lleida ('Gala Brookfield'). Shading net was removed 5 DAS. For each parameter, the mean values  $\pm$  SE ( $n = 4$ ) followed by different letters express significant differences between treatments within each day (a and b), or between days within each treatment (A and B), after Tukey's HSD test ( $p$ -value  $\leq 0.05$ ). No letters indicate a  $p$ -value  $> 0.05$ . SN-Shading net; MET-Metamitron, DAS-Days after spraying.

	Starch ( $\text{mg g}^{-1}$ DW)							
	2 DAS		4 DAS		6 DAS		9 DAS	
CTR	10.5 $\pm$ 1.7	aA	8.6 $\pm$ 2.1	aA	11.0 $\pm$ 4.2	aA	3.4 $\pm$ 2.0	aB
SN	3.2 $\pm$ 0.7	bB	2.6 $\pm$ 0.9	bB	7.3 $\pm$ 2.1	aA	3.8 $\pm$ 1.3	aB
MET	3.9 $\pm$ 0.6	bA	2.1 $\pm$ 0.9	bA	4.9 $\pm$ 0.9	aA	5.3 $\pm$ 1.9	aA
MET + SN	4.8 $\pm$ 2.1	bA	2.2 $\pm$ 0.5	bA	8.0 $\pm$ 3.7	aA	2.6 $\pm$ 0.7	aA

### 3.6. Leaf Oxidative Status

#### 3.6.1. Lipid Peroxidation

The MDA and  $\text{H}_2\text{O}_2$  content were not affected regardless of treatment, as compared to CTR values (Figure 5).

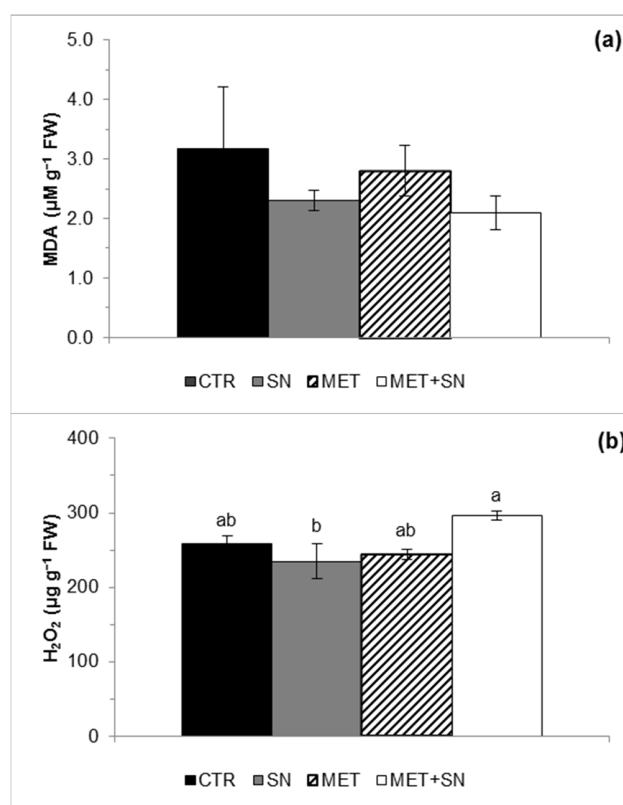


**Figure 5.** Leaf average contents of malondialdehyde (MDA) ( $\mu\text{M g}^{-1}$  FW) (a) and hydrogen peroxide ( $\text{H}_2\text{O}_2$ ) ( $\mu\text{g g}^{-1}$  FW) (b) evaluated 5 DAS, in the trial of 2018 in Sint-Truiden ('Golden Delicious'). For each parameter, the mean values  $\pm$  SE ( $n = 4$ ) followed by different letters express significant differences between treatments within each cultivar after a Tukey's HSD test ( $p$ -value  $\leq 0.05$ ). No letters indicate  $p$ -value  $> 0.05$ . SN-Shading net; MET-Metamitron.

#### 3.6.2. Antioxidative Enzyme Activity

Changes in the activity of the studied antioxidative enzymes were observed 5 DAS, differently among treatments (Figure 6). MET promoted greater activity values in APX, whereas MET + SN

induced maximal values for CAT, GR, and GPX. By contrast, these two treatments resulted in the lowest activity of SOD. POD activity differed significantly in SN (decreased) and MET (increased). The SN imposition did not significantly affect the activity of any of the studied enzymes.

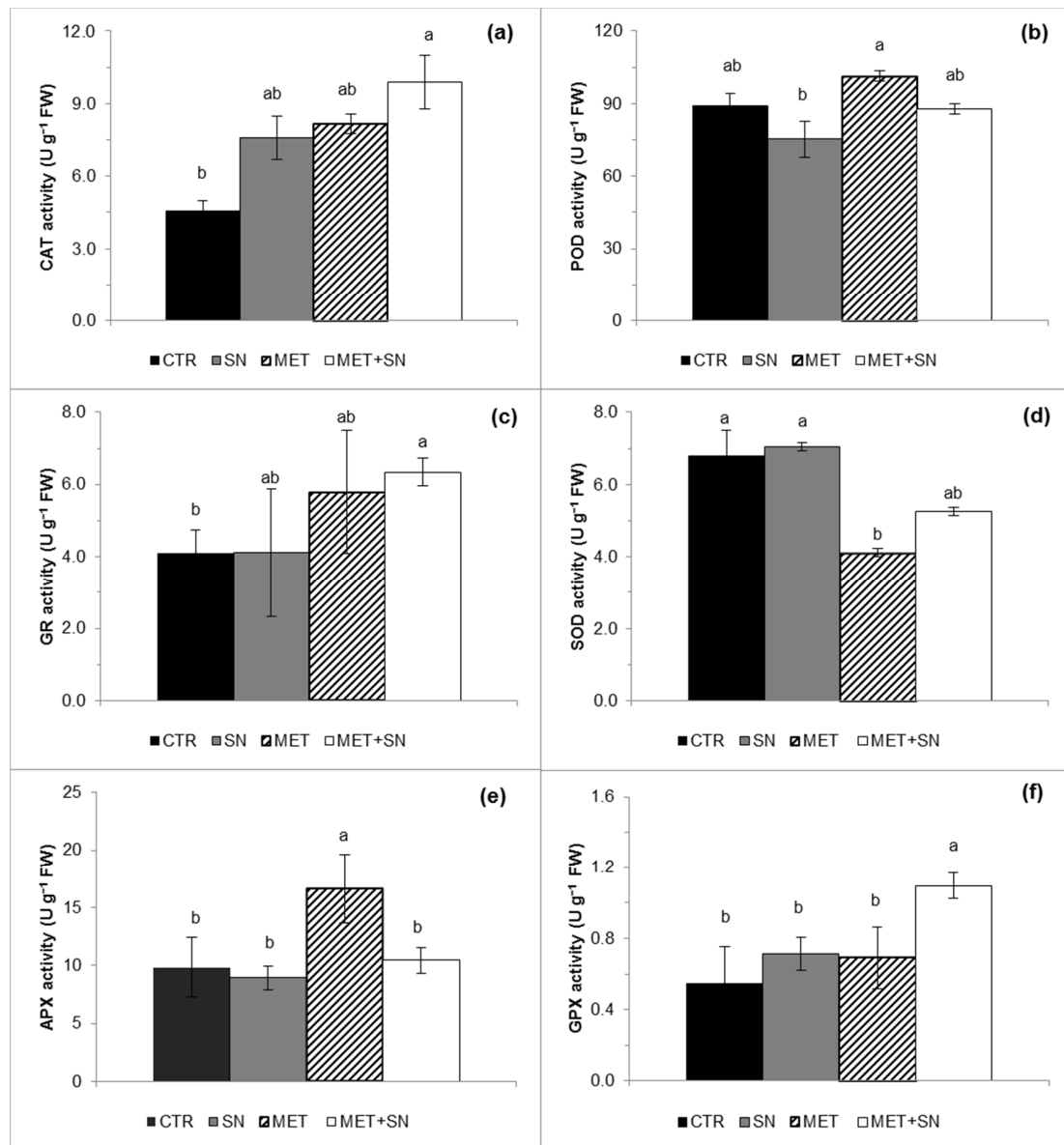


**Figure 6.** Catalase (CAT) (a), guaiacol peroxidase (POD) (b), glutathione reductase (GR) (c), superoxide dismutase (SOD) (d), ascorbate peroxidase (APX) (e) and glutathione peroxidase (GPX) (f) activities ( $\text{U g}^{-1}$  FW) evaluated 5 DAS in the trial of 2018, in Sint-Truiden ('Golden Delicious'). For each parameter, the mean values  $\pm$  SE ( $n = 4$ ) followed by different letters express significant differences between treatments within each cultivar after a Tukey's HSD test ( $p$ -value  $\leq 0.05$ ). SN-Shading net; MET-Metamitron.

### 3.6.3. Ascorbate and Glutathione Content

More than 90% of the total glutathione (GSH + GSSG) was in the reduced form (GSH) in all treatments (Figure 7a). All treatments promoted the increase of GSH + GSSG and GSH contents, significantly in MET, and, especially, MET + SN with maximal values (3 fold higher than CTR content).

Ascorbate showed a somewhat inverse pattern of that displayed by glutathione. All treatments reduced AsA and AsA + DHA contents, with minimal values observed under SN and MET + SN (Figure 7b).

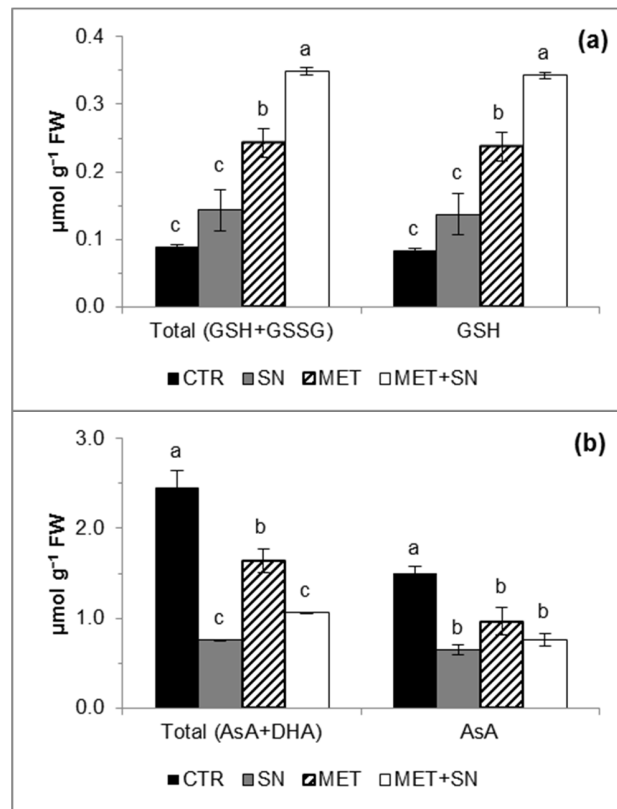


**Figure 7.** Total glutathione (GSH + GSSG) and reduced glutathione (GSH) (a) and total ascorbate (AsA + DHA) and reduced ascorbate (AsA) (b) ( $\mu\text{mol g}^{-1}$  FW) evaluated 5 DAS in the trial of 2018, in Sint-Truiden ('Golden Delicious'). For each parameter, the mean values  $\pm$  SE ( $n = 4$ ) followed by different letters express significant differences between treatments within each cultivar after a Tukey's HSD test ( $p$ -value  $\leq 0.05$ ). SN-Shading net; MET-Metamitron.

### 3.7. Yield Parameters

The MET treatment caused a consistent reduction in the number of fruits per 100/flowers clusters, although always non-significantly, whereas fruit weight and the percentage fruits  $> 70$  mm followed an opposite tendency (the latter significantly only in Girona, 2018 with a 2.7 fold increase (Table 5). Despite these changes, yield per tree was barely affected by MET.

The SN treatment induced the exact same pattern as MET, although with strong (significant) variations in fruits per 100/flowers (Girona and Sint-Truiden in 2018), fruit weight (Lleida 2017; Sint-Truiden, 2018), percentage of larger fruits (Lleida, 2017), and a somewhat stronger negative impact on yield (significantly in Sint-Truiden in 2018).

Among treatments, the MET + SN combination resulted in the greatest impacts in the studied parameters. That was the case of the reduction in fruits per 100/flowers in all trials, although significant only in Girona and Sint-Truiden in 2018. Consequently, there was a maximal significant increase in fruit weight, ranging from 20.1 g (Lleida 2017) to 109.3 g (Girona 2018), and fruit size, between 23% (Lleida, 2017), to more than double (Girona, 2017; Lleida and Girona, 2018) in all trials.

A significant reduction the yield per tree was registered only in Girona in 2018, with a decline of 58% as compared to the respective control.

**Table 5.** Number of fruits per 100 flower clusters, fruit weight (g), yield per tree (kg) and percentage of fruits in fruit size class >70 mm at harvest in the trials of 2017, in Lleida ('Gala Brookfield') and Girona ('Golden Reinders') and in the trials of 2018, in Lleida ('Gala Brookfield'), Girona ('Golden Reinders') and Sint-Truiden ('Golden Delicious'). Shading nets were removed 5 DAS. In 2017  $\pm$  SE ( $n = 16$ ) represent the average of 9–10 and 13–14 mm trials and in 2018 values  $\pm$  SE ( $n = 8$ ) represent each trial. Values followed by different letters express significant differences between treatments for each trial independently after a Tukey's HSD test ( $p$ -value  $\leq 0.05$ ). No letters indicate  $p$ -value  $> 0.05$ . SN-Shading net; MET-Metamitron.

		Fruits/100 Flower Clusters	Average Fruit Weight (g)		Yield/Tree (kg)	% Fruits > 70 mm	
<b>2017</b>							
Lleida	CTR	108.0 $\pm$ 9.8	135.5 $\pm$ 3.5	b	42.0 $\pm$ 3.4	40.5 $\pm$ 3.0	b
	SN	87.1 $\pm$ 6.0	152.9 $\pm$ 3.6	a	37.5 $\pm$ 2.6	56.0 $\pm$ 2.7	a
	MET	97.3 $\pm$ 5.0	145.9 $\pm$ 4.6	ab	39.9 $\pm$ 1.7	50.0 $\pm$ 3.5	ab
	MET + SN	84.9 $\pm$ 7.0	155.6 $\pm$ 4.3	a	36.3 $\pm$ 3.3	50.0 $\pm$ 4.1	a
Girona	CTR	184.3 $\pm$ 13.4	103.8 $\pm$ 1.4	b	21.5 $\pm$ 0.6	12.8 $\pm$ 2.0	b
	SN	173.3 $\pm$ 10.0	111.5 $\pm$ 4.4	b	19.3 $\pm$ 0.9	27.6 $\pm$ 4.3	a
	MET	169.0 $\pm$ 21.7	116.6 $\pm$ 4.2	ab	21.6 $\pm$ 0.9	27.4 $\pm$ 5.2	a
	MET + SN	163.0 $\pm$ 24.3	134.1 $\pm$ 7.9	a	20.4 $\pm$ 0.8	27.5 $\pm$ 7.1	a
<b>2018</b>							
		Fruits/100 Flower Clusters	Average Fruit Weight (g)		Yield/Tree (kg)	% Fruits > 70 mm	
Lleida	CTR	71.8 $\pm$ 11.4	125.8 $\pm$ 2.4	b	48.0 $\pm$ 6.1	48.3 $\pm$ 8.4	b
	SN	63.6 $\pm$ 5.7	133.5 $\pm$ 6.9	b	44.5 $\pm$ 3.8	73.4 $\pm$ 12.7	b
	MET	68.5 $\pm$ 4.1	132.8 $\pm$ 4.0	b	47.8 $\pm$ 2.8	58.0 $\pm$ 10.8	b
	MET + SN	47.3 $\pm$ 6.4	156.0 $\pm$ 2.3	a	37.8 $\pm$ 3.8	114.8 $\pm$ 9.8	a
Girona	CTR	121.5 $\pm$ 13.9	125.0 $\pm$ 2.7	b	36.5 $\pm$ 2.4	34.0 $\pm$ 3.3	b
	SN	49.8 $\pm$ 12.7	199.5 $\pm$ 18.8	ab	23.3 $\pm$ 5.8	83.0 $\pm$ 6.5	a
	MET	79.5 $\pm$ 13.9	197.8 $\pm$ 9.5	ab	32.5 $\pm$ 1.6	90.3 $\pm$ 2.2	a
	MET + SN	33.0 $\pm$ 11.7	234.3 $\pm$ 28.5	a	15.5 $\pm$ 4.7	89.0 $\pm$ 9.0	a
Sint-Truiden	CTR	99.0 $\pm$ 6.2	141.0 $\pm$ 6.3	c	27.5 $\pm$ 1.3	51.8 $\pm$ 9.3	b
	SN	57.5 $\pm$ 8.9	176.8 $\pm$ 7.2	ab	20.0 $\pm$ 2.5	51.8 $\pm$ 2.5	b
	MET	81.3 $\pm$ 8.4	154.3 $\pm$ 8.5	bc	24.5 $\pm$ 1.8	63.0 $\pm$ 8.2	ab
	MET + SN	41.5 $\pm$ 4.2	191.8 $\pm$ 6.1	a	24.5 $\pm$ 1.1	81.0 $\pm$ 4.0	a

## 4. Discussion

### 4.1. Influence of Irradiance on Metamitron Absorption

Herbicide absorption and susceptibility is highly dependent on climatic conditions, namely radiation [46], which can also inactivate growth regulators such as 2,4-D and indol-3-acetic acid by photolysis [47]. Metamitron is a selective herbicide which can be inactivated by a deamination reaction [48]. This reaction consists in slight modifications in the compound, associated with the rupture of the N-NH<sub>2</sub> bond, which occurs in the presence of light, oxygen, and water. This forms deaminated compounds as main degradation metabolites, mainly desamino-metamitron, which is no longer capable of inhibiting the photosystem activity [49,50]. Since metamitron maximum absorption wavelength is 306 nm, direct photodegradation reaction can occur in the field [51], in accordance with our findings that showed a higher metamitron content (Figure 2) and lower (and more stable) degradation (assessed by desamino-metamitron content) (Figure 3) in the leaves under shade (MET + SN) than under full sun exposure (MET).



#### 4.2. Effect on Gas Exchanges and RuBisCO Activity

The  $P_n$  of leaves of trees under control conditions were in line with the findings of [52], which reported values within the range between 15 and 25  $\mu\text{mol CO}_2 \text{ m}^{-2} \text{ s}^{-1}$  in apple tree leaves. PPFD is crucial to photosynthetic performance and, consequently, to photo-regulation of plant growth and development. If on one side MET disrupts the photosynthetic apparatus functioning, ultimately interrupting  $\text{CO}_2$  fixation, on the other side light deprivation (SN) would reduce light energy availability and, therefore, ATP and NADPH production.

Considerable thinning results can be obtained by shading the trees during a specific post-bloom period [8,9,53], likely resulting from carbon starvation caused by the reduction in light availability. A significantly lower total hourly net carbon exchange rate was recorded previously [8] in shaded apple trees during the 8th day shading period and observed an almost complete recovery after the nets were removed, which agrees with our results that demonstrated a strong  $P_n$  decline in SN, and a prompt recovery of C-assimilation at 6 DAS (just one day after shade removal), and an absence of effects at 10 DAS. Moreover, RuBisCO  $V_t$  did not show differences from CTR values at 5 DAS, even with the shading nets in place, what would help to support the quick  $P_n$  recovery at 6 DAS.

Metamitron can reduce  $P_n$  with a linear dose response in 'Golden Delicious' trees (the higher the concentration the greater the inhibition and the longer period for recover) [14]. In a study conducted previously [54], in 'Maxi Gala' and 'Fuji Suprema', at 3 DAS,  $P_n$  decreased 19.5% and 45.7% with very high metamitron doses of 800 and 1050 ppm, respectively. In our study, using a commercial dose of 247.5 ppm,  $P_n$  was reduced between 25 and 79% from 2 to 6 DAS (Figure 4), when  $P_n$  was still greatly suppressed. In fact, in our study, MET treated plants showed a  $P_n$  fully recovery only 10 DAS, while in a previous [54] trial, that happened already 8 DAS. However,  $g_s$  was reduced to ca. half 4 DAS using the 247.5 ppm dose, whereas an impact was observed only with 1050 ppm in 1000 L  $\text{ha}^{-1}$  in [54]. Furthermore, RuBisCO inhibition of to less than half of the control value (5 DAS) would have also contributed to the strong impact in  $P_n$  by MET.

MET + SN treatment led to minimal  $P_n$  and  $g_s$  values 2 DAS, and to an incomplete recovery 10 DAS. This treatment imposed a restriction of light energy availability, while reduced  $g_s$  and inhibited RuBisCO activity. RuBisCO activity together with a reduction of thylakoid electron transport [55], contributed to the observed  $P_n$  limitation.

#### 4.3. Effect on Non-Structural Carbohydrates

Fruit abscission is triggered by a shortage in carbohydrate content [8,56–58]. In this context, attempts to develop models aiming to support the grower in the thinning decision have been made [19,22,59,60]. Variability in thinner efficacy is related to both the stage of fruit development, and the availability of carbohydrates to support fruit growth [20]. Metamitron application was made between 9–14 mm in fruit diameter, which has been proved to be the most critical and sensitive time [61]. In fact, fruit growth is mostly dependent on tree reserves in their initial growth stage, but from the 10-mm stage onwards, become dependent on shoot photosynthesis [59,62–64]. In this way, the reduced  $P_n$ , caused either by metamitron and/or by shade, would have reduced the carbohydrate availability needed for fruit growth, justifying variations in non-structural sugar content [23].

A study conducted by [65] showed leaf sucrose and sorbitol contents by 105 to 112 DAFB, close to our values under control. In addition, taking into account the differences that result from sampling in different periods within the season (cultivar, weather, soil, and the tree conditions), our quantitative results of glucose and sorbitol (around 30 DAFB) are consistent with the work developed by other researchers [66].

Notably, with a few exceptions, glucose and fructose remained usually stable, even with the lower  $P_n$  induced by MET + SN, irrespective of location or day. These reducing sugars are involved in primary metabolism, but they did not respond to any source and sink manipulations, such as girdling and defoliation [18,66–68]. By contrast, leaf sucrose and sorbitol were mostly reduced in all treatments. Sucrose is formed in the cytoplasm and is then exported from source leaves to sink tissues [69]. Sorbitol

is the most abundant non-structural sugar in the Rosaceae family and is a major phloem-transported sugar [65–68,70]. The single, and particularly, the combined imposition of shade and metamiltron, led to reductions of sucrose and sorbitol content. In agreement, researchers [71] reported a reduction in fruit carbohydrates between 15 and 35% as compared to CTR, by shading limbs or whole trees, with a PPFD reduction of 92% for a range between 5 to 10 days.

Starch can be formed as an end product of photosynthesis in chloroplasts, being a primary storage form that can be mobilized in case of need [69,72]. In the present work, starch content was reduced 2 and 4 (and partially by 6) DAS in all treatments, likely associated with the lowered  $P_n$  values, and to a remobilization of the available starch molecules to the global metabolism.

#### 4.4. Oxidative Stress and Antioxidative Response

By interrupting thylakoid electron transport, metamiltron might promote the transfer of electrons to alternative acceptors, as molecular oxygen [27,28]. Hydroxyl radicals generated from  $H_2O_2$  have been shown to be potent inhibitors of PSII function [73–76]. However, shade would reduce the flux of photons reaching the antenna, which can decrease the oxidative conditions, as reflected in the absence of MDA and  $H_2O_2$  variation of all treatments as compared to the control (Figure 5). In apple trees subjected to abiotic stresses, as progressing drought, the increased enzymatic activity and more reduced redox state of glutathione during the acclimation period were considered an initial stress response due to changes in the redox state [77]. Here, MDA and  $H_2O_2$  values did not show significant changes in comparison with control regardless of treatment (Figure 5), and only the MET (APX) and MET + SN (CAT and GPX) promoted moderate activity increases (Figure 6). APX was slightly more active in MET treatment, what might have conferred some protection, as observed by [78], when abiotic stresses were imposed to trees. However, APX and CAT rises were not reflected in the  $H_2O_2$  levels, even considering that SOD activity and AsA contents were decreased by 5 DAS (Figure 7). Furthermore, the values of APX and GR activity obtained in this work, along with total AsA and GSH, are generally significantly lower than the ones that [79] obtained and lower than MDA and SOD results of another study [80], both obtained in apple leaves. On the other side, our  $H_2O_2$  and POD values are higher than the ones obtained previously [80]. The triggering of these antioxidative components is often observed under oxidative stress conditions. Therefore, overall, our findings pointed that increased oxidative stress conditions were not present in neither of the applied treatments.

#### 4.5. Environmental Conditions and Metamiltron Thinning Efficacy

In general, the results of 2017 and 2018 showed that the SN treatment has a stronger impact in yield related parameters (fruits/100 flower clusters, average fruit weight, yield/tree and % fruits > 70 mm) than the single metamiltron application. The number of fruits per 100 clusters was reduced by MET and/or SN (reducing radiation by 50% in the whole tree canopy for 5 days) treatments, between 6 and 42% in fruit drop, depending on year, location and treatment (stronger in MET + SN). These results in SN treatment were in close agreement with the strong fruit abscission of 90% induced by shading of the whole tree to 50% of normal light for 4 days from 20 to 41 DAFB [81]. Decreases of 35% in the number of fruits after reducing radiation by 40% during 12 days at 12-mm fruit diameter in ‘Golden’ trees [14] of 23% more fruit abscission using a 90% radiation reduction for 8 days [8] were also found. Furthermore, it was registered a reduction of 50% of the crop load in ‘Gala Must’ trees with a 70% radiation reduction for a larger period of 14 days at the stage of 14- to 26-mm fruit diameter [53], and heavy abscission rates with radiation decrease to 4% during three days [59]. Finally, after reducing 90% of irradiance for 77 daylight hours in cv. ‘Gala Mondial’, researchers [9] observed a 27% reduction in the number of fruits as compared with control.

Metamiltron application (247.5 ppm) on ‘Golden’ trees, at 12-mm fruit diameter, led to crop load reductions between 12 and 41% in trials performed previously [14], while the combination of shading nets and metamiltron led to the highest crop load reduction (40% less fruits than in control). Our results show that metamiltron, shade, and their combination increasingly reduced the number of

fruits. However, since these treatments concomitantly promoted an increase in the number (and their %) of larger size fruits (>70 mm), that resulted in the absence of significant yield reductions in most trials, except in Girona (SN) and Sint-Truiden (MET + SN), both in 2018. Researchers [71] sprayed terbacil, a photosynthesis inhibitor, and concluded that shading leads to more fruit drop comparing to the compound application, although, in the present study, the SN and MET treatments did not show significant differences in any of the trials.

In 2017, initial fruit set was low resulting in a higher difficulty to create a negative carbohydrate balance and finally, low thinning efficacies, even in MET + SN. However, in 2018, initial fruit set was very high and higher night-time temperature during the 5 nights before application (in Girona) and some cloudy days during the 3 days after (in the tree locations) might have potentiated the reduction in photoassimilates needed for fruit growth [82]. This might have contributed to some over-thinning with MET + SN treatment, which promoted abscission rates of 58% in Sint-Truiden and above 70% in Girona, responsible by a 58% cut in yield in the latter. Taking these observations together, it was clear that the extent of metamitron effect can be amplified by a lowered PPFD reaching the leaf surface. However, by comparing 2017 to 2018, other factors than low radiation that also reduce carbohydrates availability [61], such as other meteorological conditions like high night-time temperature, might contribute to increase metamitron thinning efficacy. This highlights the importance of weather conditions at the moment of imposing the treatments and in the following days, regardless of the use of shade or a chemical agent.

## 5. Conclusions

Shading net and/or metamitron application significantly limited C-assimilation, (associated with reduced  $g_s$  and RuBisCO  $V_t$ ), with after effects observed until 10 DAS.

Low radiation seems to increase metamitron absorption and/or reduce its degradation, likely resulting in a stronger and longer effect, associated to sucrose and sorbitol decreases, leading to a negative carbohydrate balance. Thus, low radiation and/or metamitron created a transient carbohydrate stress in the tree that resulted in activation of the fruit abscission zone, with a stronger abscission effect under their combined imposition (MET + SN).

Only moderate increases were observed as regards the antioxidant enzymes in MET (APX) or MET + SN (CAT, GR, GPX), accompanied by increased GSH content. Additionally, leaf lipoperoxidation and  $H_2O_2$  content remained unaltered, indicating that these metabolic defense mechanisms were able to keep oxidative stress conditions controlled.

The single use of these thinning agents can restrict the photosynthetic metabolism and sugar content, promoting thinning and the increase in fruit weight and size (fruits > 70 mm), without significant negative implications to fruit yield. However, their combination can promote an over-thinning (in Girona and Sint-Truiden, 2018), due to a further reduction of light irradiance due to cloudy days, what may lead to significant yield losses (in Girona, 2018). Therefore, thinning efficacy is also clearly dependent of environmental conditions at the time of the treatment's implementation which are of extreme importance for the achievement of an optimal thinning goal.

**Author Contributions:** Conceptualization: J.B. and L.A., and C.M.O.; Data Curation: N.R., G.À., J.C., and W.V.; Funding acquisition: J.C.R., L.A., and C.M.O.; Investigation: N.R., G.À., J.C., and W.V.; Methodology: W.V., L.A., and C.M.O.; Project administration: C.M.O.; Resources: A.B.d.S., L.L.M., M.P.M., L.C.C., and P.S.-C.; Validation: I.P.P., A.B.d.S., L.L.M., M.P.M., L.C.C., P.S.-C., and J.C.R.; Supervision: J.C.R., L.A., and C.M.O.; Writing—Original Draft: N.R.; Writing—critical review & editing, J.C.R. and C.M.O. All authors have read and agreed to the published version of the manuscript.

**Funding:** This study was supported by ADAMA-Israel, as well as by Fundação para a Ciência e a Tecnologia (FCT) through the research units UID/AGR/04129/2020 (LEAF), UIDB/00239/2020 (CEF), UIDP/04035/2020 (GeoBioTec), and UID/Multi/04046/2019 (BioISI).

**Conflicts of Interest:** The authors declare no conflict of interest.

## References

1. Food and Agriculture Organization of The United Nations. Available online: [www.faostat.fao.org](http://www.faostat.fao.org) (accessed on 18 March 2020).
2. Lakso, A.N.; Robinson, T.L.; Goffinet, M.C.; White, M.D. Apple fruit growth responses to varying thinning methods and timing. *Acta Hort.* **2001**, *557*, 407–412. [[CrossRef](#)]
3. Robinson, T.L.; Lakso, A.N. Between year and within year variation in chemical fruit thinning efficacy of apple during cool springs. *Acta Hort.* **2004**, *636*, 283–294. [[CrossRef](#)]
4. Abbaspoor, M.; Teicher, H.B.; Streibig, J.C. The effect of root-absorbed PSII inhibitors on Kautsky curve parameters in sugar beet. *Weed Res.* **2006**, *46*, 226–235. [[CrossRef](#)]
5. Guidi, L.; Degl'Innocenti, E. Imaging of Chlorophyll a Fluorescence: A Tool to Study Abiotic Stress in Plants. In *Abiotic Stress in Plants—Mechanisms and Adaptations*; Shanker, A., Ed.; InTech Open: London, UK, 2011; ISBN 978-953-307-394-1.
6. Maxwell, K.; Johnson, G.N. Chlorophyll fluorescence—A practical guide. *J. Exp. Bot.* **2000**, *51*, 659–668. [[CrossRef](#)] [[PubMed](#)]
7. Domingos, S.; Nobrega, H.; Raposo, A.; Cardoso, V.; Soares, I.; Ramalho, J.C.; Leitão, A.E.; Oliveira, C.M.; Goulão, L.F. Light management and gibberellic acid spraying as thinning methods in seedless table grapes (*Vitis vinifera* L.): Cultivar responses and effects on the fruit quality. *Sci. Hort.* **2016**, *201*, 68–77. [[CrossRef](#)]
8. Zibordi, M.; Domingos, S.; Corelli Grappadelli, L. Thinning apples via shading: An appraisal under field conditions. *J. Hort. Sci. Biotech.* **2009**, *84*, 138–144. [[CrossRef](#)]
9. Peifer, L.; Otnad, S.; Kunz, A.; Damerow, L.; Blanke, M. Effect of non-chemical crop load regulation on apple fruit quality, assessed by the DA-meter. *Sci. Hort.* **2020**, *233*, 526–531. [[CrossRef](#)]
10. Flore, J.A.; Lakso, A.N. Environmental and physiological regulation of photosynthesis in fruit crops. *Hortic. Rev.* **1989**, *11*, 111–157. [[CrossRef](#)]
11. Byers, R.; Carbaugh, D.; Presley, C.; Wolf, T. The influence of low light levels on apple fruit abscission. *J. Hort. Sci.* **1991**, *66*, 1–17. [[CrossRef](#)]
12. Lakso, A.; Grapadelli, L.C. Implications of pruning and training practices to carbon partitioning and fruit development in apple fruit. *J. Hort. Sci.* **1992**, *70*, 389–394. [[CrossRef](#)]
13. Elsasy, M.; Serra, S.; Schwallier, P.; Musacchi, S.; Einhorn, T. Net enclosure of 'Honeycrisp' and 'Gala' apple trees at different bloom stages affects fruit set and alters seed production. *Agronomy* **2019**, *9*, 478. [[CrossRef](#)]
14. Brunner, P. Impact of metamitron as a thinning compound on apple plants. *Acta Hort.* **2014**, *1042*. [[CrossRef](#)]
15. Hansen, P. Levels of sorbitol in bleeding sap and in xylem sap in relation to leaf mass and assimilate demand in apple trees. *Physiol. Plant* **1978**, *42*. [[CrossRef](#)]
16. Rees, T. Sucrose metabolism. In *Storage Carbohydrates in Vascular Plants: Distribution, Physiology and Metabolism*; Lewis, D.H., Ed.; Cambridge University Press: Cambridge, UK, 1984; pp. 53–76, ISBN 0521236983.
17. Escobar-Gutiérrez, A.J.; Gaudillere, J.P. Distribution, metabolism and role of sorbitol in higher plants: A review. *Agronomie* **1996**, *16*, 281–298.
18. Loescher, W.; Marlow, G.; Kennedy, R. Sorbitol metabolism and sink-source interconversions in developing apple leaves. *Plant Physiol.* **1982**, *70*, 335–339. [[CrossRef](#)]
19. Lakso, A.; Johnson, R. A simplified dry matter production model for apple using automatic programming simulation software. Modelling in Fruit Research II. *Acta Hort.* **1990**, *276*, 141–148. [[CrossRef](#)]
20. Robinson, T.R.; Lakso, A.N. Advances in predicting chemical thinner response of apple using a carbon balance model. *N. Y. Fruit Q.* **2011**, *19*, 15–20. [[CrossRef](#)]
21. Robinson, T.L.; Lakso, A.N.; Greene, D. Precision crop load management: The practical implementation of physiological models. *Acta Hort.* **2017**, *1177*, 381–390. [[CrossRef](#)]
22. Lordan, J.; Reginato, G.H.; Lakso, A.N.; Francescato, P.; Robinson, T.L. Natural fruitlet abscission as related to apple tree carbon balance estimated with the Malusim model. *Sci. Hort.* **2019**, *247*, 296–309. [[CrossRef](#)]
23. Robinson, T.L.; Lakso, A.N.; Greene, D.; Reginato, G.; De R. Rufato, A. Managing fruit abscission in apple. XXIX IHC—Proc. Int. Symposia on Abscission Processes in Horticulture and Non-Destructive Assessment of Fruit Attributes. *Acta Hort.* **2016**, *1119*. [[CrossRef](#)]
24. Lafer, G. Effects of chemical thinning with metamitron on fruit set, yield and fruit quality of 'Elstar'. Proceedings of XIth International Symposium on Plant Bioregulators in Fruit Production. *Acta Hort.* **2010**, *884*, 531–536. [[CrossRef](#)]

25. Penzel, M.; Kröling, C. Thinning efficacy of metamiltrone on young 'RoHo 3615' (Evelina®) apple. *Sci. Hortic.* **2020**, *272*, 1–6. [[CrossRef](#)]
26. Bechtold, U.; Field, B. Molecular mechanisms controlling plant growth during abiotic stress. *J. Exp. Bot.* **2018**, *69*, 2753–2758. [[CrossRef](#)] [[PubMed](#)]
27. Foyer, C.H.; Noctor, G. Oxygen processing in photosynthesis: Regulation and signaling. *New Phytol.* **2000**, *146*, 359–388. [[CrossRef](#)]
28. Noctor, G.; Gomez, L.; Vanacker, H.; Foyer, C.H. Interactions between biosynthesis, compartmentation and transport in the control of glutathione homeostasis and signaling. *J. Exp. Bot.* **2002**, *53*, 1283–1304. [[CrossRef](#)] [[PubMed](#)]
29. Fortunato, A.S.; Lidon, F.C.; Batista-Santos, P.; Leitão, A.E.; Pais, I.P.; Ribeiro, A.I.; and Ramalho, J.C. Biochemical and molecular characterization of the antioxidative system of *Coffea* sp. under cold conditions in genotypes with contrasting tolerance. *J. Plant Physiol.* **2010**, *167*, 333–342. [[CrossRef](#)]
30. Sharma, P.; Jha, A.B.; Dubey, R.S.; Pessarakli, M. Reactive oxygen species, oxidative damage, and antioxidative defense mechanism in plants under stressful conditions. *J. Bot.* **2012**, *2012*. [[CrossRef](#)]
31. Lesueur, C.; Knittl, P.; Gartner, M.; Mentler, A.; Furhacker, M. Analysis of 140 pesticides from conventional farming foodstuff samples after extractions with the modified QuEChERS method. *Food Control* **2008**, *19*, 906–914. [[CrossRef](#)]
32. Perchorowicz, J.T.; Raynes, D.A.; Jensen, R.G. Measurement and preservation of the in vivo activation of ribulose 1,5-bisphosphate carboxylase in leaf extracts. *Plant Physiol.* **1982**, *69*, 1165–1168. [[CrossRef](#)]
33. Ramalho, J.C.; Rodrigues, A.P.; Smedo, J.N.; Pais, I.P.; Martins, L.D.; Simões-Costa, M.C.; Leitão, A.E.; Fortunato, A.S.; Batista-Santos, P.; Palos, I.M.; et al. Sustained photosynthetic performance of *Coffea* spp. under long-term enhanced [CO<sub>2</sub>]. *PLoS ONE* **2013**, *8*. [[CrossRef](#)]
34. Stitt, M.; Bulpin, P.; Rees, T. Pathway of starch breakdown in photosynthetic tissues of *Pisum sativum*. *Biochim. Biophys.* **1978**, *544*, 200–214. [[CrossRef](#)]
35. Demiral, T.; Turkan, I. Comparative lipid peroxidation, antioxidant defense system and proline content in roots of two rice cultivars differing in salt tolerance. *Environ. Exp. Bot.* **2005**, *53*, 247–257. [[CrossRef](#)]
36. Singh, R.P.; Banerjee, S.; Kumar, P.V.S.; Raveesha, K.A.; Rao, A.R. *Tinospora Cordifolia* induces enzymes of carcinogen/drug metabolism and antioxidant system and inhibits lipid peroxidation in mice. *Phytomedicine* **2006**, *13*, 74–84. [[CrossRef](#)]
37. Aebi, H.E. Catalase. In *Methods of Enzymatic Analysis*; Bergmeyer, H.U., Ed.; Elsevier: Amsterdam, The Netherlands, 1983; Volume 2, pp. 273–286, ISBN 978-0-12-091302-2.
38. Gajewska, E.; Sklodowska, M.; Slaba, M.; Mazur, J. Effect of nickel on antioxidative enzyme activities, proline and chlorophyll contents in wheat shoots. *Biol. Plant* **2006**, *50*, 653–659. [[CrossRef](#)]
39. Shanker, A.K.; Djanaguiran, M.; Sudhagar, R.; Chandrashekar, C.N.; Pathmanabhan, G. Differential antioxidative response of ascorbate glutathione pathway enzymes and metabolites to chromium speciation stress in green gram (*Vigna radiata* (L.) R. Wilczek. cv. CO4) roots. *Plant Sci.* **2004**, *166*, 1035–1043. [[CrossRef](#)]
40. Rubio, M.; González, E.; Minchin, F.; Webb, J.; Arrese-Igor, C.; Ramos, J.; Becana, M. Effects of water stress on antioxidant enzymes of leaves and nodules of transgenic alfalfa overexpressing superoxide dismutases. *Physiol. Plant* **2002**, *115*, 531–540. [[CrossRef](#)] [[PubMed](#)]
41. Sharma, P.; Dubey, R.S. Ascorbate peroxidase from rice seedlings: Properties of enzyme isoforms. Effect of stresses and protective roles of osmolytes. *Plant Sci.* **2004**, *167*, 541–550. [[CrossRef](#)]
42. Aravind, P.; Prasad, M.N.V. Modulation of cadmium-induced oxidative stress in *Ceratophyllum demersum* by zinc involves ascorbate-glutathione cycle and glutathione metabolism. *Plant Physiol. Biochem.* **2005**, *43*, 107–116. [[CrossRef](#)]
43. Anderson, J.; Chevone, B.; Hess, J. Seasonal variation in the antioxidant system of eastern white pine needles: Evidence for thermal dependence. *Plant Physiol.* **1992**, *98*, 501–508. [[CrossRef](#)]
44. Okamura, M. An improved method for determination of L-ascorbic acid and L-dehydroascorbic acid in blood plasma. *Clin. Chim. Acta* **1980**, *103*, 259–268. [[CrossRef](#)]
45. Carvalho, L.C.; Amâncio, S. Antioxidant defense system in plantlets transferred from in vitro to ex vitro: Effects of increasing light intensity and CO<sub>2</sub> concentration. *Plant Sci.* **2002**, *162*, 33–40. [[CrossRef](#)]
46. Varanasi, A.; Vara Prasad, P.; Jugulam, M. Impact of climate change factors on weeds and herbicide efficacy. In *Advances in Agronomy*; Sparks, D.L., Ed.; Elsevier: London, UK, 2016; pp. 107–138.
47. Hollósy, F. Effects of ultraviolet radiation on plant cells. *Micron* **2002**, *33*, 179–197. [[CrossRef](#)]

48. Schmidt, R.; Fedtke, C. Metamitron activity tolerant and susceptible plants. *Pestic. Sci.* **1977**, *8*, 611–617. [[CrossRef](#)]
49. Palm, W.; Millet, M.; Zetzsch, C. Photochemical reaction of metamitron. *Chemosphere* **1997**, *35*, 1117. [[CrossRef](#)]
50. Kouras, S. Photoréactivité de la Métamitrone et Mécanisme de Photosensibilisation par le Mélange Riboflavine/Substances Humiques. Ph.D. Thesis, Faculté des Sciences Exactes, Université Mentour, Constantine, Algeria, 18 April 2012.
51. Cox, L.; Hermosin, M.; Comejo, J.; Mansour, M. Photolysis of metamitron in water in the presence of soils and soil components. *Chemosphere* **1996**, *33*, 2057–2064. [[CrossRef](#)]
52. Avery, D. Maximum photosynthetic rate—A case study in apple. *New Phytol.* **1977**, *78*, 55–63. [[CrossRef](#)]
53. Basak, A. Efficiency of fruitlet thinning in apple ‘Gala Must’ by use of metamitron and artificial shading. *J. Fruit Ornament. Plant Res.* **2011**, *19*, 51–62.
54. Gabardo, G.; Kretzschmar, A.; Petri, J.; Couto, M.; Hawerth, F.; Silva, C. Taxa fotossintética em macieiras tratadas com metamitron. *Rev. Elet. Cient. UERGS* **2017**, *3*, 617–633. [[CrossRef](#)]
55. Cheng, L.; Fuchigami, L.; Breen, P.J. The relationship between photosystem II efficiency and quantum yield for CO<sub>2</sub> assimilation is not affected by nitrogen content in apple leaves. *J. Exp. Bot.* **2001**, *52*, 1865–1872. [[CrossRef](#)]
56. Eccher, G.; Botton, A.; Dimauro, M.; Boschetti, A.; Ruperti, B.; Ramina, A. Early induction of apple fruitlet abscission is characterized by an increase of both isoprene emission and abscisic acid content. *Plant Physiol.* **2013**, *161*, 1952–1969. [[CrossRef](#)]
57. Sawicki, M.; Barka, E.; Clément, C.; Vaillant-Gaveau, N.; Jacquard, C. Cross-talk between environmental stresses and plant metabolism during reproductive organ abscission. *J. Exp. Bot.* **2015**, *66*, 1707–1719. [[CrossRef](#)] [[PubMed](#)]
58. Ackerman, M.; Samach, A. Doubts regarding carbohydrates shortage as a trigger toward abscission of specific apple (*Malus domestica*) fruitlets. *New Negat. Plant Sci.* **2015**, *1*, 46–52. [[CrossRef](#)]
59. Lakso, A.; White, M.; Tustin, D. Simulation modeling of the effects of short and long-term climatic variations on carbon balance of apple trees. *Acta Hort.* **2001**, *557*, 473–480. [[CrossRef](#)]
60. Doerflinger, F.; Lakso, A.; Braun, P. Adapting MaluSim apple tree model for the ‘Gala’ cultivar. Proc. IXth IS on Modelling in Fruit Research and Orchard Management. *Acta Hort.* **2015**, *1068*, 267–271. [[CrossRef](#)]
61. Gonzalez, L. Metamitrona, Una Nueva Herramienta Para Optimizar el Aclareo Químico en Manzano. Ph.D. Thesis, Universitat de Lleida, Lleida, Spain, 2019.
62. Byers, R.E.; Lyons, C.G.; Yoder, K.S.; Barden, J.A.; Young, R.W. Peach and apple thinning by shading and photosynthetic inhibition. *J. Hort. Sci.* **1985**, *60*, 465–472. [[CrossRef](#)]
63. Byers, R.; Barden, J.; Polomski, R.; Young, R.; Carbaugh, D. Apple thinning by photosynthetic inhibition. *J. Am. Soc. Sci.* **1990**, *115*, 14–19. [[CrossRef](#)]
64. Grapadelli, L.C.; Lakso, A.; Flore, J. Early season patterns of carbohydrate partitioning in exposed and shaded apple branches. *J. Am. Soc. Hort. Sci.* **1994**, *199*, 596–603. [[CrossRef](#)]
65. Klages, K.; Donnison, H.; Wunsche, J.; Boldingh, H. Diurnal changes in non-structural carbohydrates in leaves, phloem exudate and fruit in ‘Braeburn’ apple Functional Plant Biology. *Aust. J. Plant Physiol.* **2001**, *28*, 131–139. [[CrossRef](#)]
66. Naschitz, S.; Naor, A.; Genish, S.; Wolf, S.; Goldschmidt, E. Internal management of non-structural carbohydrate resources in apple leaves and branch wood under a broad range of sink and source manipulations. *Tree Physiol.* **2010**, *30*, 715–727. [[CrossRef](#)]
67. Wang, Z.; Pan, Q.; Quebedeaux, B. Carbon partitioning into sorbitol, sucrose, and starch in source and sink apple leaves as affected by elevated CO<sub>2</sub>. *Environ. Exp. Bot.* **1999**, *41*, 39–46. [[CrossRef](#)]
68. Mcqueen, J.; Minchin, P.; Silvester, W. Changes in non-structural carbohydrate concentration in 1-year-old shoots of ‘Braeburn’ apple (*Malus domestica*) over two consecutive years. *N. Z. J. Crop. Hort. Sci.* **2004**, *32*, 319–323. [[CrossRef](#)]
69. Zhou, R.; Quebedeaux, B. Changes in photosynthesis and carbohydrate metabolism in mature apples leaves in response to whole plant source-sink manipulation. *J. Am. Hort. Sci.* **2003**, *128*, 113–119. [[CrossRef](#)]
70. Wang, Z.; Quebedeaux, B.; Stutte, G. Osmotic adjustment: Effect of water stress on carbohydrates in leaves, stems and roots of apple. *Aust. J. Plant Physiol.* **1995**, *22*, 747–754. [[CrossRef](#)]
71. Polomski, R.F. Apple Fruit Nonstructural Carbohydrates and Abscission as Influenced by Shade and Terbacil. Master’s Thesis, Faculty of the Virginia Polytechnic Institute, Blacksburg, Virginia, 1986.

72. Breen, K.; Tustin, S.; Palmer, J.; Boldingh, H.; Close, D. Revisiting the role of carbohydrate reserves in fruit set and early-season growth of apple. *Sci. Hortic.* **2020**, *261*. [[CrossRef](#)]
73. Asada, K. Mechanisms for scavenging reactive molecules generated in chloroplasts under light stress. In *Photoinhibition of Photosynthesis—From Molecular Mechanisms to the Field*; Baker, N.R., Bowyer, J.R., Eds.; BIOS Scientific Publishers Ltd.: Oxford, UK, 1994; pp. 129–142.
74. Jakob, B.; Heber, U. Photoproduction and detoxification of hydroxyl radicals in chloroplasts and leaves and relation to photoinactivation of photosystems I and II. *Plant Cell Physiol.* **1996**, *37*, 629–635. [[CrossRef](#)]
75. Grace, S.C. Phenolics as antioxidants. In *Antioxidants and Reactive Oxygen in Plants*; Smirnoff, N., Ed.; Blackwell Publishing: Oxford, UK, 2005; pp. 141–168.
76. Logan, B.A. Reactive oxygen species and photosynthesis. In *Antioxidants and Reactive Oxygen in Plants*; Smirnoff, N., Ed.; Blackwell Publishing: Oxford, UK, 2005; pp. 250–267.
77. Sircelj, H.; Tausz, M.; Grill, D.; Batic, F. Biochemical responses in leaves of two apple tree cultivars subjected to progressing drought. *J. Plant Physiol.* **2005**, *163*, 1308–1318. [[CrossRef](#)]
78. Pandey, S.; Fartyal, D.; Agarwal, A.; Shakla, T.; James, D.; Kaul, T.; Negi, Y.K.; Arora, F.; Reddy, M. Abiotic stress tolerance in plants: Myriad roles of ascorbate peroxidase. *Front. Plant Sci.* **2017**, *8*, 851. [[CrossRef](#)]
79. Li, M.; Ma, F.; Shang, P. Influence of light on ascorbate formation and metabolism in apple fruits. *Planta* **2009**, *230*, 29–51. [[CrossRef](#)]
80. Wei, Z.; Gao, T.; Liang, B.; Zhao, Q.; Ma, F.; Li, C. Effects of exogenous melatonin on methylviologen-mediated oxidative stress in apple leaf. *Int. J. Mol. Sci.* **2018**, *19*, 316. [[CrossRef](#)]
81. Kondo, S.; Takahashi, Y. Effects of high temperature in the night-time and shading in the daytime on the early drop of apple fruit ‘Starking Delicious’. *J. Jpn. Soc. Hort. Sci.* **1987**, *52*, 142–150. [[CrossRef](#)]
82. Gonzalez, L.; Torres, E.; Carbó, J.; Alegre, S.; Bonany, J.; Àvila, G.; Martín, B.; Recasens, I.; Asin, L. Effect of different application rates of metmitron as fruitlet chemical thinner or thinning efficacy and fluorescence inhibition in Gala and Fuji apple. *Plant Growth Regul.* **2019**, *89*, 251–279. [[CrossRef](#)]

**Publisher’s Note:** MDPI stays neutral with regard to jurisdictional claims in published maps and institutional affiliations.



© 2020 by the authors. Licensee MDPI, Basel, Switzerland. This article is an open access article distributed under the terms and conditions of the Creative Commons Attribution (CC BY) license (<http://creativecommons.org/licenses/by/4.0/>).